



Oxygen and light determine the pathways of nitrate reduction in a highly saline lake

Nicolás Valiente^{1,2}, Franz Jirsa^{3,4}, Thomas Hein^{5,6}, Wolfgang Wanek⁷, Patricia Bonin⁸, Juan José Gómez-Alday²

5 ¹Centre for Biogeochemistry in the Anthropocene, Department of Biosciences, Section for Aquatic Biology and Toxicology, University of Oslo, PO Box 1066 Blindern, 0316 Oslo, Norway

²Biotechnology and Natural Resources Section, Institute for Regional Development (IDR), University of Castilla-La Mancha (UCLM), Campus Universitario s/n, 02071 Albacete, Spain

³Institute of Inorganic Chemistry, University of Vienna, Waehringer Strasse 42, 1090 Vienna, Austria

10 ⁴Department of Zoology, University of Johannesburg, PO Box 524, Auckland Park, 2006 Johannesburg, South Africa

⁵WasserCluster Lunz – Inter-university Center for Aquatic Ecosystem Research, Lunz am See, Dr. Carl Kupelwieser Prom. 5, 3293 Lunz/See, Austria

⁶Institute of Hydrobiology and Aquatic Ecosystem Management, Department of Water, Atmosphere and Environment, University of Natural Resources and Life Sciences, Gregor-Mendel-Str. 33, 1180 Vienna, Austria

15 ⁷Division of Terrestrial Ecosystem Research, Department of Microbiology and Ecosystem Science, University of Vienna, Althanstrasse 14, 1090 Vienna, Austria

⁸Aix-Marseille Université, CNRS, Université de Toulon, IRD, MIO UMR 110, 13288 Marseille, France

Correspondence to: Nicolas Valiente (n.v.parra@ibv.uio.no)

Abstract. Nitrate (NO_3^-) removal from aquatic ecosystems involves several microbially mediated processes including
20 denitrification, dissimilatory nitrate reduction to ammonium (DNRA), and anaerobic ammonium oxidation (anammox)
regulated by slight changes in environmental gradients. Saline lakes are prone to the accumulation of anthropogenic
contaminants, making them highly vulnerable environments to NO_3^- pollution. We investigated nitrate removal pathways in
mesocosm experiments using lacustrine, undisturbed, organic-rich sediments from Pétrola Lake (Spain), a highly saline
waterbody subject to anthropogenic NO_3^- pollution. We used the revised ^{15}N -isotope pairing technique (^{15}N -IPT) to
25 determine NO_3^- sink processes. Our results demonstrate the coexistence of denitrification, DNRA, and anammox processes,
and their contribution was determined by environmental conditions (oxygen and light). DNRA and N_2O -denitrification were
the dominant nitrogen (N) removal pathways when oxygen and/or light were present (up to 82%). In contrast, anoxia and
darkness promoted NO_3^- reduction by DNRA (52%) and N loss by anammox (28%). Our results highlight the role of
coupled DNRA-anammox, as yet has never been investigated in hypersaline lake ecosystems. We conclude that anoxia and
30 darkness favored DNRA and anammox processes over denitrification and therefore reduce N_2O emissions to the atmosphere.

1 Introduction

Nitrogen (N) is an essential component of living organisms and its availability controls the function of aquatic ecosystems. Since the invention of technical N-fixation through the Haber–Bosch process, humankind has drastically modified the global



N budget, significantly increasing the global fixed N pool and nitrous oxide (N_2O) emissions to the atmosphere (Canfield et al., 2010). Among N species, nitrate (NO_3^-) is a widespread compound responsible for water degradation due to excessive fertilizer use in agriculture (Spalding and Exner, 1993). NO_3^- accumulation can increase primary production in surface waters and, as a consequence, can trigger oxygen deficiency and promote eutrophication of surface waterbodies (Vitousek et al., 1997). Among aquatic ecosystems, saline lakes are highly vulnerable to NO_3^- pollution. These ecosystems are mainly located in closed hydrological systems from arid and semi-arid regions, which combined with low precipitation and high evaporation rates typical of arid climates, lead to accumulate and biomagnify many pollutants compared to freshwater systems (Williams, 2002).

Microbial processes are controlling the Earth's N cycle for ~2.7 billion years and have been widely studied in aquatic ecosystems. Certain microorganisms (diazotrophs) are able to fix N_2 into a biologically useful form. In shallow aquatic ecosystems, cyanobacteria often dominate benthic N_2 fixation, which is tightly linked with light availability and photosynthesis (Lu et al., 2018). Moreover, the role of cyanobacterial blooms altering N attenuation within aquatic ecosystems has been recently reported (Zilius et al., 2018). In contrast to diazotrophs, microbes performing denitrification and anaerobic ammonium oxidation (anammox) are responsible for removing fixed N by producing N_2 gas (Canfield et al., 2010).

Denitrification is considered to be the primary process of NO_3^- removal from aquatic environments whose main end product is dinitrogen gas (hereafter referred to as N_2 -denitrification) through a multi-step reduction process (Harrison et al., 2009; Fernandes et al., 2016; Kuypers et al., 2018). N_2O is an obligate intermediate of denitrification which can be also its main end product (hereafter referred to as N_2O -denitrification) and N_2O comprises an important atmospheric greenhouse gas (310 times more potent than carbon dioxide) (Trogler, 1999). However, the nitrification process (NH_4^+ oxidation to NO_3^-) is also a significant source of atmospheric N_2O as a by-product (Bremner and Blackmer, 1978; Dore et al., 1998; Löscher et al., 2012). A large diversity and potential activity of denitrifying bacteria have been previously shown for saline lakes (Kulp et al., 2007; Lipsewers et al., 2016), as well as the existence of denitrification at the field scale (Doi et al., 2004; Gómez-Alday et al., 2014). In such ecosystems, variable redox conditions and the supply of organic matter (OM) and nutrients lead to increased N_2O production by denitrification (Huttunen et al., 2003; Liu et al., 2015). In fact, N_2O reduction to N_2 seems to be a rate-limiting step during denitrification at extremely high salinities (Shapovalova et al., 2008). Denitrification is strongly affected by oxygen availability. Despite nitrous oxide reductase activity has been always considered to be inhibited already at relatively low oxygen concentrations (0.25 mg/L) (Bonin and Gilewicz, 1991), recent studies showed that Clade II N_2O reductases (NosZ), abundant in many biomes, are highly expressed and able to reduce N_2O in the presence of low O_2 concentrations (Yoon et al., 2016; Hallin et al., 2018).

Under anaerobic conditions, anammox couples ammonium (NH_4^+) oxidation to nitrite (NO_2^-) reduction to produce N_2 (Van de Graaf et al., 1995). The activity of anammox bacteria has been described in marine ecosystems (Thamdrup and Dalsgaard, 2002), including deep-sea hypersaline anoxic basins (Van der Wielen et al., 2005), and inland waters (Schubert et al., 2006; Abed et al., 2015; Roland et al., 2017). To date, only a limited number of studies have identified anammox bacteria in saline



70 systems (Yang et al., 2012; Lipssewers et al., 2016), with a totally different community structure than described in freshwater lakes (Wang et al., 2015). So far, however, very little attention has been paid to the role of anammox processes in saline lakes.

When oxygen becomes limiting or unavailable, specific microorganisms can perform dissimilatory nitrate reduction to ammonium (DNRA) to obtain energy, retaining a more assimilable N source in the system. Thereby, by supplying NH_4^+ DNRA can promote anammox (coupled DNRA-anammox) (Jensen et al., 2011). In coastal marine environments, DNRA may be as important as, or even more important than, denitrification for NO_3^- reduction (Giblin et al., 2013), even causing eutrophication of coastal ecosystems during warm periods (Bernard et al., 2015). DNRA is promoted when NO_3^- availability is low or limited regarding available electron donors (Tiedje, 1988; Van den Berg et al., 2015). Therefore, light can impact on coupled DNRA-anammox as light will enhance primary production and the production of dissolved oxygen, which can strongly reduce the coupled DNRA-anammox process. However, the role of coupled DNRA-anammox in saline lakes has not yet been investigated.

80 In addition, sediment core incubations have been frequently used to quantify denitrification, DNRA, and anammox rates by applying the ^{15}N isotope pairing technique (^{15}N -IPT) (Risgaard-Petersen et al., 2003; Roland et al., 2017). The ^{15}N -IPT was firstly applied on sediment cores to quantify N_2 production derived from denitrification (Nielsen, 1992). Since then, many studies have focused on discriminating the relative contribution of N processes using ^{15}N -IPT, including DNRA, and recently coupled DNRA-anammox (Risgaard-Petersen et al., 2003; Holtappels et al., 2011; Hsu and Kao, 2013; Robertson et al., 2019). Hence, processes such as anammox have been traditionally underestimated. Recently, a set of equations for ^{15}N -IPT have been provided allowing to estimate the contribution of nitrous oxide production by N_2O -denitrification and the contribution of DNRA to NO_3^- reduction (Song et al., 2016; Salk et al., 2017). Prior to this revised methodology, coupled DNRA–anammox was indistinguishable from denitrification based on isotope tracer experiments (Francis et al., 2007). Henceforth, these process estimates and the new IPT approaches are necessary for a complete N balance estimation.

90 Here, we tested the hypothesis that oxygen and light conditions in the water column can alter the balance between nitrate removal pathways (denitrification, DNRA, and anammox) during sediment incubations. For this purpose, we incubated lacustrine sediments from a eutrophic lake (Pétrola Lake, Spain) and applied the revised ^{15}N -IPT to confirm and quantify N-cycling rates.

2 Methods

95 2.1 Study site

Samples were collected from Pétrola Lake (38° 50' 14'' N, 1° 33' 40'' W), 35 km southwest of Albacete, Spain. Pétrola Lake is the main wetland in the endorheic Pétrola–Corral-Rubio–La Higuera Saline Complex, which covers a total area of about 275 km² and is located in the southeastern Castilla-La Mancha Region, in the High Segura river basin. Pétrola Lake is a terminal lake occupying about 1.76 km² in the lowest topographic position of the Pétrola endorheic basin (43 km²), which



100 consists mainly of Mesozoic materials (Valiente et al., 2017). The endorheic basin is located in a zone vulnerable to
eutrophication, and fertilizer use is restricted (Order 2011/7/2 CMA). The lake is shallow (maximum depth 2 m) with major
water volume oscillations depending on seasonal precipitation. The hydrofacies varies between Mg-Cl-SO₄ (early spring)
and Mg-Na-Cl-SO₄ (early fall). The piezometric level of the aquifer is close to the topographic surface. Accordingly, various
small springs and streams drain the aquifer and discharge into the lake following a radial pattern. The lake has been
105 classified as a heavily modified water body due to the inputs of agricultural pollutants as well as untreated wastewater
directly spilled from Pétrola Village. The Pétrola endorheic basin was declared vulnerable to NO₃⁻ pollution by the Regional
Government of Castilla-La Mancha in 1998. Excess of N in the lake-aquifer system is mainly derived from inorganic
synthetic fertilizers (Valiente et al., 2018).

The field survey was conducted in July 2015. The sampling site (control point 2651; Valiente et al., 2018) was located close
110 to the lake's depocenter and is not affected by direct inputs of polluted freshwater streams or wastewaters. To evaluate initial
natural conditions (NC), water samples were collected and stored at 4 °C in darkness prior to further analyses. Furthermore,
sediment cores (n=3) were taken from the upper 20 cm lacustrine sediment using acrylic coring tubes (5 cm inner diameter,
20 cm length). Coring tubes were capped at top and bottom with silicone rubber stoppers, cooled, and transported to the
laboratory. Once there, the top 5 cm of each core was sliced and used for inorganic N-species extraction. Afterwards, these
115 slices were then frozen at -20 °C for further analysis.

Mesocosm preparation for core incubations was adapted from previous works (Welti et al., 2012). For this purpose, acrylic
mesocosms (40 cm in length, 20 cm in diameter, containing a total volume of 12.6 L) were used for sampling and incubation
to guarantee minimal disturbance of the sediment during sampling (n=9). The mesocosm tubes were acid-prewashed and
then drilled into the sediment down to approximately 20 cm depth. Then, mesocosms were filled with 2 L of lake water to
120 maintain sediment saturation during transport. Additional lake water was collected from the sampling point and stored at 4
°C to fill the mesocosms in the lab. Black plastic sheets were used to cover the mesocosms to prevent light penetration
during transport.

2.2 Sediment incubations

In the lab, the remaining volume of each mesocosm was filled with lake water (approximately 4 L), avoiding an air space
125 over the water column. All mesocosms were sealed gas-tight. The bottom of each mesocosm was firmly sealed with a plate
bolted to the mesocosm tube. The top screw cap was equipped with two holes: one to inject air or argon, and the other to
collect samples from the water column. To maintain oxic conditions in the water column, air was bubbled using an air
compressor connected to a Teflon tube (7 mm inner diameter). From this tube, branches were connected to each mesocosm
using a rubber cap. The end of each tube was assembled with a glass Pasteur pipette and placed in the upper water column.
130 For argon bubbling, a 25 L gas cylinder (Carbueros Metalicos, Spain) with a pressure regulator was used. The argon
connection to each mesocosm was similar to that used for air bubbling.



For sample collection, a Teflon tube (4 mm inner diameter) was installed through the hole using a rubber cap. The tube inlet was placed 1 cm over the sediment surface, whereas the tube outlet was closed to the atmosphere with a three-way valve. In order to maintain water circulation inside each mesocosm, a small pump was installed in the inner wall. Mesocosms were placed in a temperature-controlled room (25 °C) with no exposure to direct sunlight.

Three different treatments were studied in triplicate. Treatment 1 (OL; oxygen + light) mimicked field conditions by means of atmospheric air bubbling, to provide oxygen, and normal dark-light cycles (~ 14 h of light per day; no additional light source was used). Mesocosms of treatment 1 (n=3) were placed close to the room window. OL is henceforth considered as control. For treatment 2 (OD; oxygen + darkness), oxic conditions in the water column were preserved via atmospheric air bubbling. However, each mesocosm was covered with aluminum foil to protect it from light. Finally, treatment 3 (AD; anoxia + darkness) maintained anoxic conditions by bubbling argon and mesocosms were shielded from light. The bubbling fluxes applied in the experiments were established based on the maximum solubility values of N₂ (Hamme and Emerson, 2004) and N₂O (Weiss and Price, 1980) in seawater using a salinity value of 50 g/L, similar to the one previously reported in Pétroula Lake (Valiente et al., 2018). Mesocosms were stabilized in the laboratory until constant N-NO₃⁻ and N-NO₂⁻ concentrations in the water column were reached. During the stabilization period, physico-chemical parameters, and inorganic N-species were monitored at 12 h intervals, starting 12 h after collection of the sediment cores (time -36), and finishing 48 h after field sampling (time 0).

In order to apply the ¹⁵N-IPT approach to quantify NO₃⁻ transformation processes inside the mesocosms, ¹⁵N-labeled nitrate (K¹⁵NO₃) was added once mesocosm stabilization was reached (time 0). This involved spiking with 250 μmol of ¹⁵N-NO₃, reaching a water column concentration of about 40 μM N-NO₃⁻. After labeled nitrate addition, the sampling frequency and incubation times were calculated following the NICE handbook (Dalsgaard et al., 2000). Thus, 30 min intervals were adopted as the initial sampling rate: this was calculated as the optimal time to enable denitrification to reach 90% of its steady state value, assuming a sediment penetration depth of oxygen of 1 mm based on previous works (Valiente et al., 2017).

In each mesocosm, water samples were taken from the water column for inorganic N-species and N-isotope analysis (N-NO₃⁻, N-NH₄⁺, N₂, and N₂O) at times 0, 0.5, 1, 1.5, 2, 2.5, 3, 4, 5, 6, 8, 10, 12, 15, 18, 24, 30, 36, 48, 60, and 72 h with a 50 mL syringe. Moreover, water samples for physico-chemical analyses, dissolved organic carbon (DOC), and dissolved bound nitrogen (DNb) determination were collected at times 0.5, 2, 4, 8, 12, 24, 48, and 72 h from each collecting Teflon tube using a 50 mL syringe. At the end of the incubations, sediment samples were obtained from the upper 5 cm of each mesocosm, homogenized using a spatula, and used fresh for chemical analyses. Sediment samples were frozen (-20 °C) before further analyses.

2.3 Physico-chemical analyses

Physico-chemical parameters measured included temperature, pH, electrical conductivity (EC), total dissolved solids (TDS), redox potential (Eh), and dissolved oxygen (DO). These parameters were determined directly in the surface water from site



165 2651 using a HQ40d Portable Multi-Parameter Meter (Hach Company, USA). During sediment incubations, physico-
chemical parameters were measured in the collected water samples. Collected water samples were immediately filtered
through a 0.45 μm nylon Millipore® filter. Inorganic N-species were determined directly after collection at the Institute for
Regional Development (University of Castilla-La Mancha). Determination of NO_2^- and NO_3^- concentration was achieved by
UV-VIS spectrophotometry via the modified Griess reaction assay as described by García-Robledo et al. (2014). NH_4^+
170 concentrations were quantified by UV-VIS spectrophotometry using the modified indophenol method, as described by
Hood-Nowotny et al. (2010). Dissolved inorganic nitrogen (DIN) was calculated by summing up the concentrations of N-
 NO_2^- , N- NO_3^- , and N- NH_4^+ . DOC and DNB measurements were performed using a Shimadzu TOC-V Analyzer with a total
nitrogen measurement unit (TNM-1) at the Institute of Inorganic Chemistry of the University of Vienna, Austria. Dissolved
organic nitrogen (DON) concentrations were estimated by subtracting DIN from the measured DNB.
175 Sedimentary N- NO_3^- (S-N- NO_3^-), N- NH_4^+ (S-N- NH_4^+), and N- NO_2^- (S-N- NO_2^-) were determined after extraction from fresh
sediment following Hood-Nowotny et al. (2010). Frozen sediment samples were lyophilized for 48 h, followed by
homogenization in a porcelain mortar and sieving through a 1 mm steel sieve. Organic matter (OM) content in dried
sediment samples was determined as loss of ignition (LOI) by combustion of dried sediments for 2 h at 550 °C at the
Institute of Inorganic Chemistry of the University of Vienna, as described by Nelson and Sommers (1996).

180 **2.4 Isotope composition of N species**

The isotopic composition of N- NH_4^+ in the water column was determined by a microdiffusion method (Lachouani et al.,
2010). Sample aliquots (10 mL) were transferred to 20 mL HDPE vials with pre-weighed MgO (100 mg). Then, acid traps
were added. They trapped the ammonia gas produced from ammonium when hydration of MgO increased the pH to >9.5.
Acid traps consisted of glass fiber filter discs (5 mm in diameter) placed on a strip of Teflon tape; 5 μL 2.5 M KHSO_4 was
185 pipetted onto the filter discs and the Teflon tapes folded and closed. Microdiffusion vials were then closed and placed on an
orbital shaker at room temperature for 2 days. Subsequently, each acid trap was transferred into a 1.5 mL reaction tube.
Tubes were placed into a desiccator containing concentrated H_2SO_4 for at least 24 h until further processing. To measure the
isotopic composition of N- NO_3^- , nitrate was isolated from the previously microdiffused extracts by a reduction-
microdiffusion method after conversion by Devarda's alloy to N- NH_4^+ (Prommer et al., 2014). The recovery efficiency of the
190 conversion was expected to be $\geq 95\%$ (Sørensen and Jensen, 1991; Mulvaney et al., 1997). Immediately after adding
Devarda's alloy, a new acid trap was added to each vial to retain ammonia gas deriving from nitrate reduction; the
subsequent procedure was the same as described above. The filter discs from the acid traps were finally transferred into tin
capsules and directly analyzed for N content and at $\%^{15}\text{N}$ by EA-IRMS using an elemental analyzer (EA 1110, CE
Instruments) connected via a ConFlo III interface (Thermo Fisher) to a DELTA^{plus} IRMS (Finnigan MAT) in the SILVER
195 Lab (University of Vienna).

To measure the isotopic composition of N_2 and N_2O , water samples were collected by 60-mL plastic syringes and transferred
to gas tight vials (22 mL Exetainer Labco, High Wycombe, UK) containing 1 mL 100 mM HgCl_2 to halt biological



reactions. Each vial was completely filled with water sample avoiding any gas headspace. All vials were stored and shipped to the Mediterranean Institute of Oceanography (Aix-Marseille Université) for the analysis of N_2 ($^{29}N_2$ and $^{30}N_2$) and N_2O isotopic species concentrations ($^{44}N_2O$, $^{45}N_2O$, and $^{46}N_2O$) using GC-MS (Stevens et al., 1993). Dissolved N_2 and N_2O were extracted from the samples in the Exetainer vials by introducing a 6 mL He headspace while simultaneously removing 6 mL of sample water. Sample injection was performed using a modified head-space autosampler (TriPlus 300, Thermo Fisher) that involves gas-equilibration at 65 °C for 6 min whilst shaking vigorously, so that more than 98% of the N_2 and N_2O equilibrium concentration was attained (Weiss, 1970). GC-MS analysis was performed using an Interscience Compact GC system equipped with AS9-HC and AG9-HCT columns. The GC conditions were as follows: injector temperature, 140 °C; oven temperature, 60 °C; carrier gas flow rate, He 15 mL/min; interface temperature, 60 °C. The mass spectrometer was used in electron ionization mode, with an electron energy of 70 eV. Data were acquired in full-scan (m/z 2–200) and selected ion monitoring (SIM) mode (m/z 29, 30 monitored for N_2 ; m/z 44, 45, 46 monitored for N_2O). Ar ($m/z = 40$) was used as an internal standard. Data were acquired and analyzed using Excalibur software. Quantification of N isotopes in both gases was performed at the Mediterranean Institute of Oceanography (Aix-Marseille Université). Finally, isotopic mass balance calculations were performed using discrete time points compared to the originally added amount of $^{15}N-NO_3$. Starting from the initial amount spiked (250 $\mu\text{mol K}^{15}NO_3$), N concentrations and atom percent enrichments were used to calculate the percentage of ^{15}N recovery in specific N forms and overall.

2.5 Denitrification, DNRA, and anammox activity measurements

For ^{15}N -IPT modeling, the revised ^{15}N -IPT calculation procedure (Salk et al., 2017) was applied. A detailed description of parameters and equations is included in Table 1. For this purpose, our incubations were assumed to be intact core incubations. The probabilities of NO_3^- reduction via denitrification, DNRA, and anammox were assumed to be equal (Song et al., 2016). Genuine N_2 production via denitrification (D_{1d}) and anammox (A_{1d}), as well as N_2O production via denitrification, were calculated for each time step. Production rates were calculated according to Salk et al. (2017) for each time point after the addition of the labelled $^{15}NO_3^-$. Non-linear increments in the ^{15}N content were taken into account by calculating the N production rates (i.e. $^{15}NH_4^+$, $^{29}N_2$, $^{30}N_2$, $^{45}N_2O$, $^{46}N_2O$) from the slope of the initial time point and each specific time point rather than a slope of all time points. Thus, a total of 20 rates of each process were calculated for each mesocosm. Ratios of $^{14}NO_3^-:^{15}NO_3^-$ (r_{1d}) and $^{14}NH_4^+:^{15}NH_4^+$ (r_{1da}) were calculated and used as base parameters for activity calculations. The applied methodology allowed distinguishing between N_2 production via coupled DNRA-anammox and via canonical anammox. DNRA rates were calculated using the production of $^{15}NH_4^+$, and of $^{30}N_2$ for anammox, over time. However, this model cannot discriminate between $^{15}NO_3^-$ assimilation and subsequent remineralization of OM to $^{15}NH_4^+$, and DNRA. Thus, the DNRA rate may include both processes. The sum of N_2 production by denitrification and anammox, together with N_2O production via denitrification, is designated as ‘Total N loss’. The ‘Total NO_3^- reduction’ adds the DNRA rate to the previous estimate.



230 2.6 Statistical analysis

Changes in chemistry and rates of N-loss processes over time as well as at the end of the incubation were assessed using one-way analysis of variance (ANOVA), followed by the Tukey's post hoc test (homogeneous variances) or by the Games-Howell post hoc test (heterogeneous variances). To assess differences in the hydrochemical conditions between initial (n=1) and final conditions (n=9), one-sample two-tailed t-tests were used. Results of statistical tests were considered to be
235 significant at the confidence level 95% ($\alpha = 0.05$). All tests were performed using SPSS-IBM Statistics software.

3 Results and discussion

3.1 Differences between treatments in chemical parameters and rates of N-loss processes

Differences between initial (NC₋₄₈, time -48 h) and final conditions (EX₇₂, time 72 h) were assessed for the three treatment groups (Table 2). Salinity, as TDS values, was around the hypersaline limit (50 g/L), with values ranging from 45.1 g/L (NC₋₄₈) to 50.1 g/L (AD₇₂). Concerning inorganic N-species in the water column, the final N-NO₃⁻ and N-NO₂⁻ concentrations were below the limit of detection (LOD, <0.05 μ M). N-NH₄⁺ concentrations increased significantly (t-test, $p < 0.05$) between
240 NC₋₄₈ and final conditions in OL₇₂ ($t_{(2)} = 8.33$), OD₇₂ ($t_{(2)} = 17.89$) and AD₇₂ ($t_{(2)} = 19.23$). Furthermore, there was a significant effect of light on the N-NH₄⁺ concentration ($F_{(2,6)} = 15.98$). Tukey's post hoc tests indicated that the final N-NH₄⁺ concentration in OL₇₂ ($139 \pm 15.7 \mu\text{mol/L}$) was significantly lower than in OD₇₂ ($175 \pm 10.9 \mu\text{mol/L}$) and AD₇₂ ($198 \pm 12.2 \mu\text{mol/L}$). N₂ and N₂O final concentrations (time 72 h) did not show significant differences between treatments ($F_{(2,6)}$ of 0.55 and 0.54, respectively).

DOC concentrations increased significantly between NC₋₄₈ and final conditions in OL₇₂ ($t_{(2)} = 6.30$) and OD₇₂ ($t_{(2)} = 9.89$) but not in AD₇₂ ($t_{(2)} = 3.79$). Between treatments, there were no significant differences in DOC ($F_{(2,6)} = 0.91$). DNb and DON concentrations did not change over time ($p > 0.05$), and did not differ between treatments ($F_{(2,6)}$ of 1.28 and 0.95,
250 respectively). The contribution of DON to DNb (DON:DNb) decreased significantly between NC₋₄₈ and final conditions in all treatments (OL₇₂, $t_{(2)} = -26.4$; OD₇₂, $t_{(2)} = -6.89$; AD₇₂, $t_{(2)} = -8.28$), and differed between treatments ($F_{(2,6)} = 5.31$). Values of pH (OL₇₂, $t_{(2)} = -17.14$; OD₇₂, $t_{(2)} = -10.26$; AD₇₂, $t_{(2)} = -6.43$) and Eh (OL₇₂, $t_{(2)} = -7.81$; OD₇₂, $t_{(2)} = -8.88$; AD₇₂, $t_{(2)} = -5.15$) decreased significantly between NC₋₄₈ and final conditions in the three treatments. Between treatments, only pH showed significant differences ($F_{(2,6)} = 5.37$). In the sediment samples, LOI ($F_{(3,8)} = 0.50$) and S-N-NH₄⁺ ($F_{(3,8)} = 3.54$) did not differ
255 ($p > 0.05$) between NC₋₄₈ and final conditions or between treatments. Significant differences were found in S-N-NO₃⁻ concentrations over time ($F_{(3,8)} = 7.81$), but not between treatments.

Regarding N-loss processes, mean (\pm standard deviation) and maximum rates are presented in Table 3, whereas a complete record of rates can be found in the Supplementary Information (Table S1). Among treatments, significant differences were only found for DNRA ($F_{(2,161)} = 10.0$). Games-Howell post hoc tests indicated DNRA depends on oxygen in the water



260 column, distinguishing between AD ($2.80 \pm 2.56 \text{ mmol N m}^{-2} \text{ h}^{-1}$) and OL ($1.54 \pm 1.53 \text{ mmol N m}^{-2} \text{ h}^{-1}$) or OD (1.35 ± 1.20
 $\text{mmol N m}^{-2} \text{ h}^{-1}$) treatments.

Within each treatment, significant differences were found over time among processes. DNRA and N_2O -denitrification showed significant time-related differences in the OL treatment ($F_{(5,47)}$ of 5.70 and 3.82, respectively). These processes, together with N_2 -anammox in the interval 3-6 h of incubation, were shown as the dominant ones according to Game-Howell
265 post hoc tests. In the OD treatment, significant differences among processes were found in the interval 3-24 h of incubation. At that time, DNRA and N_2O -denitrification rates differed from the other processes ($F_{(5,49)}$ of 6.89 and 3.53, respectively). Games-Howell post hoc tests showed that DNRA was the dominant process in the OD treatment between 3 and 6 h of incubation, and then, up to 24 h of incubation, DNRA was co-dominant with N_2O -denitrification. Finally, significant differences were found in the AD treatment between DNRA and the other processes from 3 h of incubation onwards ($F_{(5,50)} =$
270 3.32). Games-Howell post hoc tests indicated that DNRA was the dominant process up to 48 h.

3.2 Hydrogeochemical dynamics during sediment incubations

Three different treatments were applied during sediment incubations by modifying oxygen and light conditions in the water column (see Table 2 for details). The evolution of N parameters is shown in Figure 1 (N-species) and Figure 2 (^{15}N). In Figure 1, the evolution of N-NO_3^- and N-NO_2^- showed a well-defined nitrate-reduction pattern in all treatments. N-NO_3^-
275 concentrations decreased to below the limit of detection during the first stage (S1) in all treatments. Immediately after tracer addition, N-NO_3^- increased markedly and then gradually decreased (stage S2), the decline being fastest in the AD treatment (anoxia and darkness). This trend was also observed in Figure 2: $^{15}\text{NO}_3^-$ reached maximum concentrations at 6 h (OL treatment), 12 h (OD treatment), and 1 h (AD treatment), and was completely removed from the water column within the first 36 h (OL and OD) and 12 h (AD). This decrease in N-NO_3^- concentrations suggests the existence of assimilatory and/or
280 dissimilatory nitrate reduction processes.

During the final stage (S3), N-NO_3^- was below LOD, which may be the result of either the absence of complete nitrification in the water column, or the rate of NO_3^- consumption being higher than the rate of NO_3^- production. N-NO_3^- in the sediment was significantly higher at the end of the incubations in all treatments. The existence of NO_3^- reduction pathways, mainly during S2, is the most plausible explanation according to the isotopic data. However, other major issues for ^{15}N -IPT studies
285 such as uptake and intracellular storage should not be discarded (Robertson et al., 2019). Significant inputs of NO_3^- may also promote blooms of diatoms (frequent in Pétröla Lake), which are physiologically adapted to grow rapidly under nitrate-rich conditions (Bronk et al., 2007). A phytoplankton bloom was observed after $^{15}\text{N-NO}_3^-$ addition in the light treatment (OL), with a subsequent decay. Even though we cannot prove it, the role of diatom-bacteria aggregates in removing NO_3^- from the water column subsequently fueling benthic anaerobic N-cycling, should be considered (Kamp et al., 2016).

290 N-NO_2^- peaked during the second stage (S2), paralleling the decrease in N-NO_3^- (Figure 1). Subsequently, N-NO_2^- decreased faster in treatment AD than in treatments OL (oxygen and light) and OD (oxygen and darkness). The intermittent conversion of nitrate to nitrite suggests active NO_3^- reduction processes. In contrast, N-NH_4^+ in the water column increased



over time in all treatments. The concentration moderately increased during S1 in all treatments (Figure 1). From the addition of the labelled NO_3^- , concentration of N-NH_4^+ increased (with small oscillations) coupled with a constant increase in $^{15}\text{NH}_4^+$ (Figure 2) up to 18 h of incubation. This increase was more pronounced in AD than in OD and OL treatments. From 24 h until the end of the incubation, N-NH_4^+ concentration increased whereas $^{15}\text{NH}_4^+$ tended to stabilize. According to these results, N-NH_4^+ accumulation in the water column can be explained by DNRA (0 – 18 h), OM remineralization, and sedimentary NH_4^+ release (Kalvelage et al., 2013). During the S1 stage, the absence of NO_3^- hindered the activity of DNRA, and the increase of NH_4^+ in the water column must therefore be a consequence of rapid release from decaying cyanobacteria, as demonstrated by others (Gao et al., 2013). The small oscillations observed through S2 were the result of fluctuations in N-NH_4^+ production (DNRA, water-column OM remineralization) and consumption (anammox, NH_4^+ assimilation, and nitrification). Thus, NH_4^+ accumulation in the water column during S3 can be attributed to sedimentary OM remineralization after bloom collapse (García-Robledo et al., 2011), as the values did not significantly differ from initial conditions.

Concentrations of N_2 were measured from the addition of the $^{15}\text{N-NO}_3^-$. In general, Figure 1 showed a stable concentration of N_2 over time with small peaks in the first 12 h of incubation (positive for OL and AD treatments, negative for OD treatment). However, a sudden drop in N_2 concentration was found at 5 h in treatment OD, probably due to an occasional episode of N_2 stripping, even though steady state gas concentrations were kept throughout the incubations. By comparing these data with $^{15}\text{N-N}_2$ evolution data (Figure 2) small variations in both $^{29}\text{N}_2$ and $^{30}\text{N}_2$ were observed after the tracer addition, where the sharp increase of N_2 in the OD treatment at 48 h coincided with an abrupt rise in $^{30}\text{N}_2$. During the hours after the tracer addition (stage S2), the production of $^{30}\text{N}_2$ can be attributed either to denitrification or to coupled DNRA-anammox, by combining the DNRA substrate ($^{15}\text{NO}_2^-$) with the DNRA product ($^{15}\text{NH}_4^+$) (Holtappels et al., 2011). Considering N_2O evolution, a different pattern was observed than that described for N_2 . Thus, an increasing trend was observed in all three treatments (Figure 1). N_2O accumulated towards the end of the incubations in treatments OD and AD, with concentrations above 2.0 mmol/L. $^{45}\text{N}_2\text{O}$ and $^{46}\text{N}_2\text{O}$ evolution also provided evidence of N_2O -denitrification during the S2 stage, both increasing over time (Figure 2). However, once the original NO_3^- had been consumed, increases in both $^{45}\text{N}_2\text{O}$ and $^{46}\text{N}_2\text{O}$ for the oxic treatments can be attributed to other processes such as ^{15}N recirculation by coupled DNRA-nitrification (DNRA fueling nitrification to N_2O), a process whose importance has recently been highlighted in estuarine sediments (Dunn et al., 2009; Murphy et al., 2016). Finally, the solubility of N_2O at 50 g/L of salinity and 25 °C was 14.25 mmol/L, whereas the solubility for N_2 at the same conditions was significantly lower (0.43 mmol/L). Therefore, N_2 oversaturation is observed in the water column (Figure 1), clear evidence for the presence of the above-described NO_3^- reduction processes (Wenk et al., 2013; 2014). Concentrations of N_2 remained almost constant throughout the incubations (≈ 6 mmol/L), regardless of whether atmospheric air (OL and OD) or argon (AD) was bubbling in the mesocosm. Thus, N_2 oversaturation is probably the result of N reduction and further accumulation in the water column, which has not yet reached atmospheric equilibrium for nitrogen (Weiss and Craig, 1973). About $^{29}\text{N}_2$ and $^{30}\text{N}_2$ concentrations, used for the IPT calculations, they remained almost unchanged and below the maximum solubility value (Figure 2). In addition, the ^{15}N mass balance was calculated to detect whether gas bubbling (atmospheric air or argon to maintain mesocosms in an aerobic or



330 anoxic state) and differences in solubility may strip $^{29}\text{N}_2$ and $^{30}\text{N}_2$ faster than $^{45}\text{N}_2\text{O}$ and $^{46}\text{N}_2\text{O}$ (Figure 3). Mean ^{15}N recoveries were 92% for OL (from 79 to 108%), 94% for OD (from 67 to 125%), and 93% for AD (from 73 to 126 %). ^{15}N losses of 6-8% based on whole-system ^{15}N recoveries seem very small and may derive mainly from the accumulation of errors in the measurements (concentrations and $\text{at}\%^{15}\text{N}$ enrichments) of 4-5 dissolved and gaseous N pools. Therefore, we consider that there were no significant N losses deriving from gas bubbling, but if so the experiment would have only underestimated N_2 production processes (i.e. full denitrification and anammox).

335 Figure 4 shows the evolution of physico-chemical parameters. The evolution of DOC and DON in the water column showed stable concentrations during S1, followed by a sharp increase in S2 after tracer addition (Figure 4). Diatom blooms can disrupt the ecological balance, causing the breakdown of cyanobacterial populations, and the release of large amounts of dissolved OM (Xue et al., 2017). Afterwards, DOC and DON decreased as a result of heterotrophic metabolism. In S3, we explain the observed DOC changes first by consumption and finally by accumulation after bloom collapse. DON increases are likely related to phytoplankton decay with subsequent organic N mineralization. Decreasing percentages of DON:DNB underline the role of OM remineralization throughout the incubation. Compared to initial conditions, pH decreased in OL, 340 OD and AD treatments. The decrease of pH values is probably due to the release of organic acids and CO_2 , both produced from carbon sources during microbial metabolism. pH values were within the optimal range for denitrification (Knowles, 1982) and DNRA (Van den Berg et al., 2015). Eh abruptly dropped in S1 and maintained negative values during S2 and S3, with a small rise after tracer addition (Figure 4).

3.3 Nitrous oxide production

345 The contribution of each process to total N removal was calculated for each mesocosm and treatment. ANOVA results provided evidence of a (co-)dominant role of N_2O -denitrification in OL and OD treatments, with 82% and 81% of N removal, respectively (Figure 5). Contribution of N_2O -denitrification to total N loss was significantly higher than reported for aquatic sediments ($< 8.6\%$; Risgaard-Petersen et al., 2003; McCrackin and Elser, 2010). Treatments OL and OD showed mean N_2O -denitrification rates of $1.76 (\pm 2.58)$ and $2.10 (\pm 2.24)$ $\text{mmol N m}^{-2} \text{h}^{-1}$, respectively. Such high values have been 350 reported previously only in tropical wetland soils (up to $1.56 \text{ mmol N m}^{-2} \text{h}^{-1}$; Lienggaard, et al., 2014) and estuarine sediments affected by agricultural activities (up to $4.85 \text{ mmol N m}^{-2} \text{h}^{-1}$; Salahudeen et al., 2018) (Table 4). These results support evidence from previous observations (Huttunen et al., 2003), which showed that lakes subjected to elevated N inputs are an important source of N_2O emissions. However, studies involving the role of N_2O -denitrification in saline aquatic environments are mainly restricted to marine ecosystems. Our high measured rates may be explained by the high biological activity after $^{15}\text{N-NO}_3^-$ addition, in the absence of nutrient limitation. Nonetheless, the N_2O production in field studies is 355 most probably limited by N availability. Another potential source of N_2O production is partial nitrification. In treatments OD and OL, the conditions are met for this process to take place. No NO_3^- was measured after the tracer addition and further consumption, but N_2O was produced over time. In fact, Figure 6 shows that N_2O -denitrification was the main pathway in the



S3 stage for such treatments, which may mask the contribution of nitrification fueled by DNRA. Finally, abiotic contribution
360 to N₂O production may also contribute to produce N₂O in hypersaline environments (Samarkin et al., 2010).

The AD treatment showed a similar average value of N₂O-denitrification (1.87 ± 3.99 mmol N m⁻² h⁻¹) than treatments OL
and OD, being similar to rates reported for pristine mangrove sediments (up to 0.67 mmol N m⁻² h⁻¹; Fernandes et al., 2010),
but higher rates of N₂-denitrification than OL and OD. Therefore, N₂O-denitrification showed a smaller yet still dominant
contribution to total N removal in the AD treatment. A possible explanation for this pattern is that N₂O reductase activity is
365 sensitive towards oxygen (Bonin and Gilewicz, 1991), being partially inhibited in treatments OL and OD in the presence of
dissolved O₂ (~ 6.4 mg/L in the water column), thereby decreasing N₂-denitrification in aerated treatments. Overall, N₂O-
denitrification showed a significant contribution to NO₃⁻ reduction during the whole sediment incubations together with
DNRA (Figure 6). In terms of NO₃⁻ reduction, when N₂O-denitrification was of greater importance, DNRA and anammox
showed a smaller contribution to NO₃⁻ reduction, and vice versa. As suggested above, the influence of partial nitrification as
370 a source of N₂O cannot be discarded. Unfortunately, additional experiments would have been necessary which were not the
main focus of this study (pathways of nitrate removal).

N₂-denitrification showed the highest rates at the beginning of the incubation (AD, ≤ 13 mmol N m⁻² h⁻¹). Mean measured N₂
production rates attributed to denitrification in the OL treatment was 0.05 mmol N m⁻² h⁻¹, in accordance with intact
estuarine sediments (0.036 – 0.155 mmol N m⁻² h⁻¹; Trimmer et al., 2003) and contributed on average 4% to total N removal
375 (Figure 3). N₂-denitrification played a greater role in NO₃⁻ reduction under darkness: 11% and 13% of the total N removal in
OD and AD treatments, respectively. These results agree with earlier observations (Risgaard-Petersen et al., 1994) which
showed reduced denitrification rates associated with light exposure and photosynthesis by benthic microphytes. In the OD
treatment, mean production rate was 0.41 (± 1.57) mmol N m⁻² h⁻¹ by N₂-denitrification (Table 3). Our values were similar to
those reported in marine environments like Heron Island (0.48 mmol N m⁻² h⁻¹; Eyre and Ferguson, 2008) and Randers Fjord
380 (0.34 mmol N m⁻² h⁻¹; Risgaard-Petersen et al., 2004) (Table 4). Highest N₂-denitrification rates were found in the AD
treatment with an average value of 0.80 (± 2.61) mmol N m⁻² h⁻¹. These results were close to those reported by Erler et al.
(2008) (0.652 – 0.966 mmol N m⁻² h⁻¹), where denitrifiers coexisted with anammox bacteria in a constructed wetland which
received secondary treated sewage effluents. The largest contribution of N₂-denitrification was detected at the initial stages
of incubation, coupled to higher DOC concentrations, but also during late stages of incubation in OD (~ 30%) (Figure 4).
385 These results suggest the dominance of heterotrophic denitrification linked to the breakdown of biomass (Xue et al., 2017).

3.4 Close coupling between DNRA and anammox

Total N removal and NO₃⁻ reduction reached highest values under anoxia and darkness conditions (mean of 3.63 ± 5.30
mmol N m⁻² h⁻¹ and 6.43 ± 6.56 mmol N m⁻² h⁻¹, respectively; Table 3). As discussed above, under those conditions DNRA
was the dominant process. These results are consistent with hydrochemical data, which showed a significant accumulation of
390 N-NH₄⁺ in the water column in the AD treatment.



Previous research showed favorable conditions for DNRA activity in sediments from Pétrola Lake, such as high organic C:N ratios or the presence of microorganisms capable of performing DNRA (Valiente et al., 2017; Valiente et al., 2018). Average DNRA rates in OL and OD treatments ($\sim 1.4 \text{ mmol N m}^{-2} \text{ h}^{-1}$) were similar to those reported for anoxic estuarine sediments where DNRA was the dominant process ($1.140 \text{ mmol N m}^{-2} \text{ h}^{-1}$; Dong et al., 2011). In the AD treatment, mean DNRA rates
395 ($2.80 \pm 2.56 \text{ mmol N m}^{-2} \text{ h}^{-1}$) were similar to those observed in nutrient enriched environments like fringing wetlands (up to $6.13 \text{ mmol N m}^{-2} \text{ h}^{-1}$; Tobias et al., 2011) or eutrophic shelf seas (up to $3.58 \text{ mmol N m}^{-2} \text{ h}^{-1}$; Song et al., 2013) (Table 4). In line with the data obtained in the ANOVA tests, the ^{15}N -IPT data showed that NO_3^- reduction by DNRA was significantly higher in AD (52%) than in OL (41%) and OD (35%) (Figure 5). The contribution of DNRA was in the same range as reported for estuarine and salt marsh sediments (Dong et al., 2009; Koop-Jakobsen and Giblin, 2010), fostering the retention
400 of reactive nitrogen in the system. Compared to denitrification, DNRA contributed more to NO_3^- reduction after the initial incubation phase, approximately from time 2.5 h onwards (Figure 4). Recent studies also demonstrated that DNRA is stimulated in the presence of H_2S at the expense of denitrification (Roland et al., 2017). Our results support those findings: AD provided the most favorable conditions for bacterial sulfate-reduction (Table 2), and H_2S production in Pétrola sediments (Valiente et al., 2017) can reach values up to $0.024 \text{ nmol/cm}^3\cdot\text{s}$.

405 DNRA therefore plays the key role in increasing N- NH_4^+ contents in the water column, being more relevant than OM remineralization and sedimentary release. Existing NH_4^+ may be oxidized to NO_2^- both under aerobic and anaerobic conditions (Schmidt et al., 2002), contributing to a temporary increase of N- NO_2^- and promoting NO_2^- and NH_4^+ consumption by anammox bacteria. Moreover, N- NH_4^+ release does fuel N loss from the system via coupled DNRA-anammox. Therefore, DNRA and anammox bacteria acting together may have an energetic advantage over denitrifiers in the
410 competition for substrates under low oxygen conditions (Jensen et al., 2011). The close reliance of anammox on DNRA has been reported in marine ecosystems with high N loss via anammox, mainly linked to the availability of OM (Kalvelage et al., 2013). In Pétrola Lake sediment incubations, anammox seems to be fueled by DNRA. This interpretation is based on the similar trend in the contribution of both processes to total NO_3^- reduction (AD>OL>OD; Figure 3). Coupled DNRA-anammox showed a higher contribution in all treatments than canonical anammox (Table 3), corroborating the key role of
415 DNRA in fueling N loss pathways.

The isotope data clearly confirm the presence of anammox (Table 3). The mean rates of N loss via anammox in OL and OD treatments ($\sim 0.4 \text{ mmol N m}^{-2} \text{ h}^{-1}$) were in the range of previous studies in eutrophic sediments (up to $0.413 \text{ mmol N m}^{-2} \text{ h}^{-1}$; Han and Li, 2016), but significantly lower than those found in the AD treatment ($0.96 \text{ mmol N m}^{-2} \text{ h}^{-1}$). These results agree with recent studies showing the importance of anammox activity in the presence of H_2S in freshwater lakes (Roland et al.,
420 2017), conditions which are given for the highly saline lake studied here. On average, the contribution of anammox to total N loss ranged from 8% (OD) to 28% (AD) (Figure 3). This range corresponds with studies performed in continental shelf sediments (Song et al., 2013) (28%), intertidal sediments (Hsu and Kao, 2013) (12%), and is close to the global mean value including inland waters (Trimmer and Engström, 2011) (23%). Finally, the higher the participation of anammox in total N



removal, the lower the relevance of N₂O-denitrification, leading to decreased N₂O emissions from hypersaline lake
425 ecosystems.

4 Conclusions

The purpose of the current study was to determine the influence of oxygen and light in the water column on the balance
between nitrate removal pathways during incubations of lacustrine organic-rich sediments. Our findings provide evidence for
the coexistence of denitrification, DNRA, and anammox in a highly saline lake. The application of the revised ¹⁵N-IPT
430 highlighted the importance of coupled DNRA-anammox during our incubations. We showed here that DNRA and N₂O-
denitrification played a predominant role in N removal under the studied conditions, showing unexpectedly high N₂O
emission rates compared to previous studies. However, DNRA was the key process when oxygen and light were absent from
the water column. Then, anammox also had a greater influence on total N removal with markedly high rates (up to 0.96
mmol N m⁻² h⁻¹). It seems that anoxia and darkness promoted DNRA, the critical process which fuels anammox. As a result,
435 these conditions reduced N₂O emissions to the atmosphere. As far as we know, the role of coupled DNRA-anammox in such
saline ecosystems has not yet been explored, and therefore, anammox was typically underestimated. Further research is
required to fully understand the role of coupled DNRA-anammox in N cycling in lake ecosystems, as well as the influence
that coupled DNRA-nitrification can exert on N₂O production.

Acknowledgements

440 The work was supported by a PhD grant (BES-2012-052256) and project CICYT- CGL2017-87216-C4-2-R from the
Spanish government, the SBPLY/17/180501/000296 project from the Castilla–La Mancha regional government, and funds
for a Research Visit to Vienna (UCLM). We thank M. Stachowitsch for English copyediting and valuable comments. Special
thanks to A. Menchén, B. Toledo, M. A. Gutiérrez, A. Valenciano, and A. García for their laboratory help. The authors are
also grateful for the analytical assistance to all colleagues from the Environmental and Radiochemistry Group (University of
445 Vienna), from the SILVER Lab (University of Vienna), from WasserCluster Lunz, and from the MEB Group (Aix-Marseille
Université), and to an anonymous reviewer for helpful comments and suggestions.

References

Abed, R. M. M., de Beer, D. and Stief, P.: Functional-Structural Analysis of Nitrogen-Cycle Bacteria in a Hypersaline Mat
from the Omani Desert, *Geomicrobiology Journal*, 32(2), 119–129, doi:[10.1080/01490451.2014.932033](https://doi.org/10.1080/01490451.2014.932033), 2015.



- 450 Bernard, R. J., Mortazavi, B. and Kleinhuizen, A. A.: Dissimilatory nitrate reduction to ammonium (DNRA) seasonally dominates NO₃⁻ reduction pathways in an anthropogenically impacted sub-tropical coastal lagoon, *Biogeochemistry*, 125(1), 47–64, doi:[10.1007/s10533-015-0111-6](https://doi.org/10.1007/s10533-015-0111-6), 2015.
- Bonin, P. and Gilewicz, M.: A direct demonstration of “co-respiration” of oxygen and nitrogen oxides by *Pseudomonas nautica*: some spectral and kinetic properties of the respiratory components, *FEMS Microbiology Letters*, 80(2–3), 183–188, 455 doi:[10.1111/j.1574-6968.1991.tb04658.x](https://doi.org/10.1111/j.1574-6968.1991.tb04658.x), 1991.
- Bremner, J. M. and Blackmer, A. M.: Nitrous Oxide: Emission from Soils During Nitrification of Fertilizer Nitrogen, *Science*, 199(4326), 295, doi:[10.1126/science.199.4326.295](https://doi.org/10.1126/science.199.4326.295), 1978.
- Bronk, D. A., See, J. H., Bradley, P. and Killberg, L.: DON as a source of bioavailable nitrogen for phytoplankton, *Biogeosciences*, 4(3), 283–296, doi:[10.5194/bg-4-283-2007](https://doi.org/10.5194/bg-4-283-2007), 2007.
- 460 Canfield, D. E., Glazer, A. N. and Falkowski, P. G.: The Evolution and Future of Earth’s Nitrogen Cycle, *Science*, 330(6001), 192, doi:[10.1126/science.1186120](https://doi.org/10.1126/science.1186120), 2010.
- Crowe, S. A., Treusch, A. H., Forth, M., Li, J., Magen, C., Canfield, D. E., Thamdrup, B. and Katsev, S.: Novel anammox bacteria and nitrogen loss from Lake Superior, *Scientific Reports*, 7(1), 13757, doi:[10.1038/s41598-017-12270-1](https://doi.org/10.1038/s41598-017-12270-1), 2017.
- Dalsgaard, T., Nielsen, L., Brotas, V., Viaroli, P., Underwood, G., Nedwell, D., Sundbäck, K., Rysgaard, S., Miles, A., 465 Bartoli, M. and others: Protocol handbook for NICE-Nitrogen Cycling in Estuaries: a project under the EU research programme: Marine Science and Technology (MAST III), Ministry of Environment and Energy National Environmental Research Institute, 2000.
- Doi, H., Kikuchi, E., Mizota, C., Satoh, N., Shikano, S., Yurlova, N., Yadrenkina, E. and Zuykova, E.: Carbon, nitrogen, and sulfur isotope changes and hydro-geological processes in a saline lake chain, *Hydrobiologia*, 529(1), 225–235, 470 doi:[10.1007/s10750-004-6418-2](https://doi.org/10.1007/s10750-004-6418-2), 2004.
- Dong, L. F., Smith, C. J., Papaspyrou, S., Stott, A., Osborn, A. M. and Nedwell, D. B.: Changes in Benthic Denitrification, Nitrate Ammonification, and Anammox Process Rates and Nitrate and Nitrite Reductase Gene Abundances along an Estuarine Nutrient Gradient (the Colne Estuary, United Kingdom), *Appl. Environ. Microbiol.*, 75(10), 3171, doi:[10.1128/AEM.02511-08](https://doi.org/10.1128/AEM.02511-08), 2009.
- 475 Dong, L. F., Sobey, M. N., Smith, C. J., Rusmana, I., Phillips, W., Stott, A., Osborn, A. M. and Nedwell, D. B.: Dissimilatory reduction of nitrate to ammonium, not denitrification or anammox, dominates benthic nitrate reduction in tropical estuaries, *Limnology and Oceanography*, 56(1), 279–291, doi:[10.4319/lo.2011.56.1.0279](https://doi.org/10.4319/lo.2011.56.1.0279), 2011.
- Dore, J. E., Popp, B. N., Karl, D. M. and Sansone, F. J.: A large source of atmospheric nitrous oxide from subtropical North Pacific surface waters, *Nature*, 396(6706), 63–66, doi:[10.1038/23921](https://doi.org/10.1038/23921), 1998.
- 480 Dunn, R. J. K., Welsh, D. T., Jordan, M. A., Teasdale, P. R. and Lemckert, C. J.: Influence of natural amphipod (*Victoriopisaaustraliensis*) (Chilton, 1923) population densities on benthic metabolism, nutrient fluxes, denitrification and DNRA in sub-tropical estuarine sediment, *Hydrobiologia*, 628(1), 95–109, doi:[10.1007/s10750-009-9748-2](https://doi.org/10.1007/s10750-009-9748-2), 2009.



- Erler, D. V., Eyre, B. D. and Davison, L.: The Contribution of Anammox and Denitrification to Sediment N₂ Production in a Surface Flow Constructed Wetland, *Environ. Sci. Technol.*, 42(24), 9144–9150, doi:[10.1021/es801175t](https://doi.org/10.1021/es801175t), 2008.
- 485 Eyre, B. D. and Ferguson, A. J. P.: Denitrification efficiency for defining critical loads of carbon in shallow coastal ecosystems, in *Eutrophication in Coastal Ecosystems: Towards better understanding and management strategies Selected Papers from the Second International Symposium on Research and Management of Eutrophication in Coastal Ecosystems*, 20–23 June 2006, Nyborg, Denmark, edited by J. H. Andersen and D. J. Conley, pp. 137–146, Springer Netherlands, Dordrecht., 2009.
- 490 Fernandes, S. O., Bharathi, P. A. L., Bonin, P. C. and Michotey, V. D.: Denitrification: An Important Pathway for Nitrous Oxide Production in Tropical Mangrove Sediments (Goa, India), *Journal of Environmental Quality*, 39(4), 1507–1516, doi:[10.2134/jeq2009.0477](https://doi.org/10.2134/jeq2009.0477), 2010.
- Fernandes, S. O., Javanaud, C., Michotey, V. D., Guasco, S., Anschutz, P. and Bonin, P.: Coupling of bacterial nitrification with denitrification and anammox supports N removal in intertidal sediments (Arcachon Bay, France), *Estuarine, Coastal and Shelf Science*, 179, 39–50, doi:[10.1016/j.ecss.2015.10.009](https://doi.org/10.1016/j.ecss.2015.10.009), 2016.
- 495 Francis, C. A., Beman, J. M. and Kuypers, M. M. M.: New processes and players in the nitrogen cycle: the microbial ecology of anaerobic and archaeal ammonia oxidation, *The ISME Journal*, 1(1), 19–27, doi:[10.1038/ismej.2007.8](https://doi.org/10.1038/ismej.2007.8), 2007.
- Gao, L., Zhang, L., Hou, J., Wei, Q., Fu, F. and Shao, H.: Decomposition of macroalgal blooms influences phosphorus release from the sediments and implications for coastal restoration in Swan Lake, Shandong, China, *Ecological Engineering*, 500 60, 19–28, doi:[10.1016/j.ecoleng.2013.07.055](https://doi.org/10.1016/j.ecoleng.2013.07.055), 2013.
- García-Robledo, E. and Corzo, A.: Effects of macroalgal blooms on carbon and nitrogen biogeochemical cycling in photoautotrophic sediments: An experimental mesocosm, *Marine Pollution Bulletin*, 62(7), 1550–1556, doi:[10.1016/j.marpolbul.2011.03.044](https://doi.org/10.1016/j.marpolbul.2011.03.044), 2011.
- García-Robledo, E., Corzo, A. and Paspasyrou, S.: A fast and direct spectrophotometric method for the sequential 505 determination of nitrate and nitrite at low concentrations in small volumes, *Marine Chemistry*, 162, 30–36, doi:[10.1016/j.marchem.2014.03.002](https://doi.org/10.1016/j.marchem.2014.03.002), 2014.
- GIBLIN, A. E., TOBIAS, C. R., SONG, B., WESTON, N., BANTA, G. T. and H.RIVERA-MONROY, V.: The Importance of Dissimilatory Nitrate Reduction to Ammonium (DNRA) in the Nitrogen Cycle of Coastal Ecosystems, *Oceanography*, 26(3), 124–131, 2013.
- 510 Gilbert F, Souchu P, Bianchi M and Bonin P: Influence of shellfish farming activities on nitrification, nitrate reduction to ammonium and denitrification at the water-sediment interface of the Thau lagoon, France, *Mar Ecol Prog Ser*, 151, 143–153, 1997.
- Gómez-Alday, J. J., Carrey, R., Valiente, N., Otero, N., Soler, A., Ayora, C., Sanz, D., Muñoz-Martín, A., Castaño, S., Recio, C., Carnicero, A. and Cortijo, A.: Denitrification in a hypersaline lake–aquifer system (Pétrola Basin, Central Spain): 515 The role of recent organic matter and Cretaceous organic rich sediments, *Science of The Total Environment*, 497–498, 594–606, doi:[10.1016/j.scitotenv.2014.07.129](https://doi.org/10.1016/j.scitotenv.2014.07.129), 2014.



- van de Graaf, A. A., Mulder, A., de Bruijn, P., Jetten, M. S., Robertson, L. A. and Kuenen, J. G.: Anaerobic oxidation of ammonium is a biologically mediated process., *Appl. Environ. Microbiol.*, 61(4), 1246, 1995.
- Hallin, S., Philippot, L., Löffler, F. E., Sanford, R. A. and Jones, C. M.: Genomics and Ecology of Novel N₂O-Reducing Microorganisms, *Trends in Microbiology*, 26(1), 43–55, doi:[10.1016/j.tim.2017.07.003](https://doi.org/10.1016/j.tim.2017.07.003), 2018.
- 520 Hamme, R. C. and Emerson, S. R.: The solubility of neon, nitrogen and argon in distilled water and seawater, *Deep Sea Research Part I: Oceanographic Research Papers*, 51(11), 1517–1528, doi:[10.1016/j.dsr.2004.06.009](https://doi.org/10.1016/j.dsr.2004.06.009), 2004.
- Han, H. and Li, Z.: Effects of macrophyte-associated nitrogen cycling bacteria on ANAMMOX and denitrification in river sediments in the Taihu Lake region of China, *Ecological Engineering*, 93, 82–90, doi:[10.1016/j.ecoleng.2016.05.015](https://doi.org/10.1016/j.ecoleng.2016.05.015), 2016.
- 525 Harrison, J. A., Maranger, R. J., Alexander, R. B., Giblin, A. E., Jacinthe, P.-A., Mayorga, E., Seitzinger, S. P., Sobota, D. J. and Wollheim, W. M.: The regional and global significance of nitrogen removal in lakes and reservoirs, *Biogeochemistry*, 93(1), 143–157, doi:[10.1007/s10533-008-9272-x](https://doi.org/10.1007/s10533-008-9272-x), 2009.
- Holtappels, M., Lavik, G., Jensen, M. M. and Kuypers, M. M. M.: Chapter ten - 15N-Labeling Experiments to Dissect the Contributions of Heterotrophic Denitrification and Anammox to Nitrogen Removal in the OMZ Waters of the Ocean, in *530 Methods in Enzymology*, vol. 486, edited by M. G. Klotz, pp. 223–251, Academic Press., 2011.
- Hood-Nowotny, R., Umana, N. H.-N., Inselbacher, E., Oswald- Lachouani, P. and Wanek, W.: Alternative Methods for Measuring Inorganic, Organic, and Total Dissolved Nitrogen in Soil, *Soil Science Society of America Journal*, 74(3), 1018–1027, doi:[10.2136/sssaj2009.0389](https://doi.org/10.2136/sssaj2009.0389), 2010.
- Hsu, T.-C. and Kao, S.-J.: Technical Note: Simultaneous measurement of sedimentary N₂ and N₂O production and a modified ¹⁵N isotope pairing technique, *Biogeosciences*, 10(12), 7847–7862, doi:[10.5194/bg-10-7847-2013](https://doi.org/10.5194/bg-10-7847-2013), 2013.
- 535 Huttunen, J. T., Juutinen, S., Alm, J., Larmola, T., Hammar, T., Silvola, J. and Martikainen, P. J.: Nitrous oxide flux to the atmosphere from the littoral zone of a boreal lake, *Journal of Geophysical Research: Atmospheres*, 108(D14), doi:[10.1029/2002JD002989](https://doi.org/10.1029/2002JD002989), 2003.
- Jensen, M. M., Lam, P., Revsbech, N. P., Nagel, B., Gaye, B., Jetten, M. S. and Kuypers, M. M.: Intensive nitrogen loss over the Omani Shelf due to anammox coupled with dissimilatory nitrite reduction to ammonium, *The ISME Journal*, 5(10), 540 1660–1670, doi:[10.1038/ismej.2011.44](https://doi.org/10.1038/ismej.2011.44), 2011.
- Kalvelage, T., Lavik, G., Lam, P., Contreras, S., Arteaga, L., Löscher, C. R., Oshlies, A., Paulmier, A., Stramma, L. and Kuypers, M. M. M.: Nitrogen cycling driven by organic matter export in the South Pacific oxygen minimum zone, *Nature Geoscience*, 6(3), 228–234, doi:[10.1038/ngeo1739](https://doi.org/10.1038/ngeo1739), 2013.
- 545 Kamp, A., Stief, P., Bristow, L. A., Thamdrup, B. and Glud, R. N.: Intracellular Nitrate of Marine Diatoms as a Driver of Anaerobic Nitrogen Cycling in Sinking Aggregates, *Frontiers in Microbiology*, 7, 1669, doi:[10.3389/fmicb.2016.01669](https://doi.org/10.3389/fmicb.2016.01669), 2016.
- Knowles, R.: Denitrification, *Microbiol Rev*, 46(1), 43–70, 1982.
- Koop-Jakobsen, K. and Giblin, A. E.: The effect of increased nitrate loading on nitrate reduction via denitrification and 550 DNRA in salt marsh sediments, *Limnology and Oceanography*, 55(2), 789–802, doi:[10.4319/lo.2010.55.2.0789](https://doi.org/10.4319/lo.2010.55.2.0789), 2010.



- Kulp, T. R., Han, S., Saltikov, C. W., Lanoil, B. D., Zargar, K. and Oremland, R. S.: Effects of Imposed Salinity Gradients on Dissimilatory Arsenate Reduction, Sulfate Reduction, and Other Microbial Processes in Sediments from Two California Soda Lakes, *Appl. Environ. Microbiol.*, 73(16), 5130, doi:[10.1128/AEM.00771-07](https://doi.org/10.1128/AEM.00771-07), 2007.
- Kuypers, M. M. M., Marchant, H. K. and Kartal, B.: The microbial nitrogen-cycling network, *Nature Reviews Microbiology*, 16(5), 263–276, doi:[10.1038/nrmicro.2018.9](https://doi.org/10.1038/nrmicro.2018.9), 2018.
- Lachouani, P., Frank, A. H. and Wanek, W.: A suite of sensitive chemical methods to determine the $\delta^{15}\text{N}$ of ammonium, nitrate and total dissolved N in soil extracts, *Rapid Communications in Mass Spectrometry*, 24(24), 3615–3623, doi:[10.1002/rcm.4798](https://doi.org/10.1002/rcm.4798), 2010.
- Lienggaard, L., Figueiredo, V., Markfoged, R., Revsbech, N. P., Nielsen, L. P., Prast, A. E. and Kühl, M.: Hot moments of N₂O transformation and emission in tropical soils from the Pantanal and the Amazon (Brazil), *Soil Biology and Biochemistry*, 75, 26–36, doi:[10.1016/j.soilbio.2014.03.015](https://doi.org/10.1016/j.soilbio.2014.03.015), 2014.
- Lipsewers, Y. A., Hopmans, E. C., Meysman, F. J. R., Sinninghe Damsté, J. S. and Villanueva, L.: Abundance and Diversity of Denitrifying and Anammox Bacteria in Seasonally Hypoxic and Sulfidic Sediments of the Saline Lake Grevelingen, *Frontiers in Microbiology*, 7, 1661, doi:[10.3389/fmicb.2016.01661](https://doi.org/10.3389/fmicb.2016.01661), 2016.
- 555 Liu, W., Wang, Z., Zhang, Q., Cheng, X., Lu, J. and Liu, G.: Sediment denitrification and nitrous oxide production in Chinese plateau lakes with varying watershed land uses, *Biogeochemistry*, 123(3), 379–390, doi:[10.1007/s10533-015-0072-9](https://doi.org/10.1007/s10533-015-0072-9), 2015.
- Löscher, C. R., Kock, A., Könneke, M., LaRoche, J., Bange, H. W. and Schmitz, R. A.: Production of oceanic nitrous oxide by ammonia-oxidizing archaea, *Biogeosciences*, 9(7), 2419–2429, doi:[10.5194/bg-9-2419-2012](https://doi.org/10.5194/bg-9-2419-2012), 2012.
- 570 Lu, Y., Wen, Z., Shi, D., Chen, M., Zhang, Y., Bonnet, S., Li, Y., Tian, J. and Kao, S.-J.: Effect of light on N₂ fixation and net nitrogen release of *Trichodesmium* in a field study, *Biogeosciences*, 15(1), 1–12, doi:[10.5194/bg-15-1-2018](https://doi.org/10.5194/bg-15-1-2018), 2018.
- Marchant, H. K., Holtappels, M., Lavik, G., Ahmerkamp, S., Winter, C. and Kuypers, M. M. M.: Coupled nitrification–denitrification leads to extensive N loss in subtidal permeable sediments, *Limnology and Oceanography*, 61(3), 1033–1048, doi:[10.1002/lno.10271](https://doi.org/10.1002/lno.10271), 2016.
- 575 McCrackin, M. L. and Elser, J. J.: Atmospheric nitrogen deposition influences denitrification and nitrous oxide production in lakes, *Ecology*, 91(2), 528–539, doi:[10.1890/08-2210.1](https://doi.org/10.1890/08-2210.1), 2010.
- Mulvaney, R. L., Khan, S. A., Stevens, W. B. and Mulvaney, C. S.: Improved diffusion methods for determination of inorganic nitrogen in soil extracts and water, *Biology and Fertility of Soils*, 24(4), 413–420, doi:[10.1007/s003740050266](https://doi.org/10.1007/s003740050266), 1997.
- 580 Murphy, A. E., Anderson, I. C., Smyth, A. R., Song, B. and Luckenbach, M. W.: Microbial nitrogen processing in hard clam (*Mercenaria mercenaria*) aquaculture sediments: the relative importance of denitrification and dissimilatory nitrate reduction to ammonium (DNRA), *Limnology and Oceanography*, 61(5), 1589–1604, doi:[10.1002/lno.10305](https://doi.org/10.1002/lno.10305), 2016.
- Nelson, D. W. and Sommers, L. E.: Total Carbon, Organic Carbon, and Organic Matter, in *Methods of Soil Analysis*, pp. 961–1010, John Wiley & Sons, Ltd., 2018.



- 585 Nielsen, L. P.: Denitrification in sediment determined from nitrogen isotope pairing, *FEMS Microbiology Letters*, 86(4), 357–362, doi:[10.1111/j.1574-6968.1992.tb04828.x](https://doi.org/10.1111/j.1574-6968.1992.tb04828.x), 1992.
- Prisu, J. C., Downes, M. T. and McKay, C. P.: Extreme supersaturation of nitrous oxide in a poorly ventilated Antarctic lake, *Limnology and Oceanography*, 41(7), 1544–1551, doi:[10.4319/lo.1996.41.7.1544](https://doi.org/10.4319/lo.1996.41.7.1544), 1996.
- Prommer, J., Wanek, W., Hofhansl, F., Trojan, D., Offre, P., Urich, T., Schleper, C., Sassmann, S., Kitzler, B., Soja, G. and
590 Hood-Nowotny, R. C.: Biochar decelerates soil organic nitrogen cycling but stimulates soil nitrification in a temperate arable field trial, *PLoS One*, 9(1), e86388–e86388, doi:[10.1371/journal.pone.0086388](https://doi.org/10.1371/journal.pone.0086388), 2014.
- Risgaard-Petersen, N., Rysgaard, S., Nielsen, L. P. and Revsbech, N. P.: Diurnal variation of denitrification and nitrification in sediments colonized by benthic microphytes, *Limnology and Oceanography*, 39(3), 573–579, doi:[10.4319/lo.1994.39.3.0573](https://doi.org/10.4319/lo.1994.39.3.0573), 1994.
- 595 Risgaard-Petersen, N., Nielsen, L. P., Rysgaard, S., Dalsgaard, T. and Meyer, R. L.: Application of the isotope pairing technique in sediments where anammox and denitrification coexist, *Limnology and Oceanography: Methods*, 1(1), 63–73, doi:[10.4319/lom.2003.1.63](https://doi.org/10.4319/lom.2003.1.63), 2003.
- Risgaard-Petersen, N., Rikke Louise Meyer, Markus Schmid, Mike S. M. Jetten, Alex Enrich-Prast, SÃf Åren Rysgaard and Niels Peter Revsbech: Anaerobic ammonium oxidation in an estuarine sediment, *Aquat Microb Ecol*, 36(3), 293–304,
600 2004.
- Robertson, E. K., Bartoli, M., Bruchert, V., Dalsgaard, T., Hall, P. O. J., Hellemann, D., Hietanen, S., Zilius, M. and Conley, D. J.: Application of the isotope pairing technique in sediments: Use, challenges, and new directions, *Limnology and Oceanography: Methods*, 17(2), 112–136, doi:[10.1002/lom3.10303](https://doi.org/10.1002/lom3.10303), 2019.
- Roland, F. A. E., Darchambeau, F., Borges, A. V., Morana, C., De Brabandere, L., Thamdrup, B. and Crowe, S. A.:
605 Denitrification, anaerobic ammonium oxidation, and dissimilatory nitrate reduction to ammonium in an East African Great Lake (Lake Kivu), *Limnology and Oceanography*, 63(2), 687–701, doi:[10.1002/lno.10660](https://doi.org/10.1002/lno.10660), 2018.
- Salahudeen, J. H., Reshmi, R. R., Anoop Krishnan, K., Ragi, M. S. and Vincent, S. G. T.: Denitrification rates in estuarine sediments of Ashtamudi, Kerala, India, *Environmental Monitoring and Assessment*, 190(6), 323, doi:[10.1007/s10661-018-6698-z](https://doi.org/10.1007/s10661-018-6698-z), 2018.
- 610 Salk, K. R., Erler, D. V., Eyre, B. D., Carlson-Perret, N. and Ostrom, N. E.: Unexpectedly high degree of anammox and DNRA in seagrass sediments: Description and application of a revised isotope pairing technique, *Geochimica et Cosmochimica Acta*, 211, 64–78, doi:[10.1016/j.gca.2017.05.012](https://doi.org/10.1016/j.gca.2017.05.012), 2017.
- Samarkin, V. A., Madigan, M. T., Bowles, M. W., Casciotti, K. L., Priscu, J. C., McKay, C. P. and Joye, S. B.: Abiotic nitrous oxide emission from the hypersaline Don Juan Pond in Antarctica, *Nature Geoscience*, 3(5), 341–344,
615 doi:[10.1038/ngeo847](https://doi.org/10.1038/ngeo847), 2010.
- Schmidt, I., Sliemers, O., Schmid, M., Cirpus, I., Strous, M., Bock, E., Kuenen, J. G. and Jetten, M. S. M.: Aerobic and anaerobic ammonia oxidizing bacteria – competitors or natural partners?, *FEMS Microbiology Ecology*, 39(3), 175–181, doi:[10.1111/j.1574-6941.2002.tb00920.x](https://doi.org/10.1111/j.1574-6941.2002.tb00920.x), 2002.



- Schubert, C. J., Durisch-Kaiser, E., Wehrli, B., Thamdrup, B., Lam, P. and Kuypers, M. M. M.: Anaerobic ammonium
620 oxidation in a tropical freshwater system (Lake Tanganyika), *Environmental Microbiology*, 8(10), 1857–1863,
doi:[10.1111/j.1462-2920.2006.01074.x](https://doi.org/10.1111/j.1462-2920.2006.01074.x), 2006.
- Shapovalova, A. A., Khijniak, T. V., Tourova, T. P., Muyzer, G. and Sorokin, D. Y.: Heterotrophic denitrification at
extremely high salt and pH by haloalkaliphilic Gammaproteobacteria from hypersaline soda lakes, *Extremophiles*, 12(5),
619–625, doi:[10.1007/s00792-008-0166-6](https://doi.org/10.1007/s00792-008-0166-6), 2008.
- 625 Song, G. D., Liu, S. M., Marchant, H., Kuypers, M. M. M. and Lavik, G.: Anammox, denitrification and dissimilatory nitrate
reduction to ammonium in the East China Sea sediment, *Biogeosciences*, 10(11), 6851–6864, doi:[10.5194/bg-10-6851-2013](https://doi.org/10.5194/bg-10-6851-2013),
2013.
- Song, G. D., Liu, S. M., Kuypers, M. M. M. and Lavik, G.: Application of the isotope pairing technique in sediments where
anammox, denitrification, and dissimilatory nitrate reduction to ammonium coexist, *Limnology and Oceanography*:
630 *Methods*, 14(12), 801–815, doi:[10.1002/lom3.10127](https://doi.org/10.1002/lom3.10127), 2016.
- Sørensen, P. and Jensen, E. S.: Sequential diffusion of ammonium and nitrate from soil extracts to a polytetrafluoroethylene
trap for ^{15}N determination, *Analytica Chimica Acta*, 252(1), 201–203, doi:[10.1016/0003-2670\(91\)87215-S](https://doi.org/10.1016/0003-2670(91)87215-S), 1991.
- Stevens, R. J., Laughlin, R. J., Atkins, G. J. and Prosser, S. J.: Automated Determination of Nitrogen-15-Labeled Dinitrogen
and Nitrous Oxide by Mass Spectrometry, *Soil Science Society of America Journal*, 57(4), 981–988,
635 doi:[10.2136/sssaj1993.03615995005700040017x](https://doi.org/10.2136/sssaj1993.03615995005700040017x), 1993.
- Tan, E., Zou, W., Jiang, X., Wan, X., Hsu, T.-C., Zheng, Z., Chen, L., Xu, M., Dai, M. and Kao, S.: Organic matter
decomposition sustains sedimentary nitrogen loss in the Pearl River Estuary, China, *Science of The Total Environment*, 648,
508–517, doi:[10.1016/j.scitotenv.2018.08.109](https://doi.org/10.1016/j.scitotenv.2018.08.109), 2019.
- Thamdrup, B. and Dalsgaard, T.: Production of N_2 through Anaerobic Ammonium Oxidation Coupled to Nitrate Reduction
640 in Marine Sediments, *Appl. Environ. Microbiol.*, 68(3), 1312, doi:[10.1128/AEM.68.3.1312-1318.2002](https://doi.org/10.1128/AEM.68.3.1312-1318.2002), 2002.
- Tiedje, J. M.: Ecology of Denitrification and Dissimilatory Nitrate Reduction to Ammonium, *Biology of Anaerobic
Microorganisms*, 179–244, 1988.
- Tobias, C. R., Iris C. Anderson, Elizabeth A. Canuel and Stephen A. Macko: Nitrogen cycling through a fringing marsh-
aquifer ecotone, *Mar Ecol Prog Ser*, 210, 25–39, 2001.
- 645 Trimmer, M. and Engström, P.: Distribution, Activity, and Ecology of Anammox Bacteria in Aquatic Environments, in
Nitrification, American Society of Microbiology. [online] Available from:
<https://www.asmscience.org/content/book/10.1128/9781555817145.ch09>, 2011.
- Trimmer, M., Nicholls, J. C. and Deflandre, B.: Anaerobic Ammonium Oxidation Measured in Sediments along the Thames
Estuary, United Kingdom, *Appl. Environ. Microbiol.*, 69(11), 6447, doi:[10.1128/AEM.69.11.6447-6454.2003](https://doi.org/10.1128/AEM.69.11.6447-6454.2003), 2003.
- 650 Trimmer, M., Nils Risgaard-Petersen, Joanna C. Nicholls and Pia Engström: Direct measurement of anaerobic
ammonium oxidation (anammox) and denitrification in intact sediment cores, *Mar Ecol Prog Ser*, 326, 37–47, 2006.



- Trogler, W. C.: Physical properties and mechanisms of formation of nitrous oxide, *Coordination Chemistry Reviews*, 187(1), 303–327, doi:[10.1016/S0010-8545\(98\)00254-9](https://doi.org/10.1016/S0010-8545(98)00254-9), 1999.
- Valiente, N., Carrey, R., Otero, N., Gutiérrez-Villanueva, M. A., Soler, A., Sanz, D., Castaño, S. and Gómez-Alday, J. J.:
655 Tracing sulfate recycling in the hypersaline Pétrola Lake (SE Spain): A combined isotopic and microbiological approach, *Chemical Geology*, 473, 74–89, doi:[10.1016/j.chemgeo.2017.10.024](https://doi.org/10.1016/j.chemgeo.2017.10.024), 2017.
- Valiente, N., Carrey, R., Otero, N., Soler, A., Sanz, D., Muñoz-Martín, A., Jirsa, F., Wanek, W. and Gómez-Alday, J. J.: A multi-isotopic approach to investigate the influence of land use on nitrate removal in a highly saline lake-aquifer system, *Science of The Total Environment*, 631–632, 649–659, doi:[10.1016/j.scitotenv.2018.03.059](https://doi.org/10.1016/j.scitotenv.2018.03.059), 2018.
- 660 van den Berg, E. M., van Dongen, U., Abbas, B. and van Loosdrecht, M. C.: Enrichment of DNRA bacteria in a continuous culture, *The ISME Journal*, 9(10), 2153–2161, doi:[10.1038/ismej.2015.26](https://doi.org/10.1038/ismej.2015.26), 2015.
- van der Wielen, P. W. J. J., Bolhuis, H., Borin, S., Daffonchio, D., Corselli, C., Giuliano, L., D’Auria, G., de Lange, G. J., Huebner, A., Varnavas, S. P., Thomson, J., Tamburini, C., Marty, D., McGenity, T. J. and Timmis, K. N.: The Enigma of Prokaryotic Life in Deep Hypersaline Anoxic Basins, *Science*, 307(5706), 121, doi:[10.1126/science.1103569](https://doi.org/10.1126/science.1103569), 2005.
- 665 Vitousek, P. M., Aber, J. D., Howarth, R. W., Likens, G. E., Matson, P. A., Schindler, D. W., Schlesinger, W. H. and Tilman, D. G.: HUMAN ALTERATION OF THE GLOBAL NITROGEN CYCLE: SOURCES AND CONSEQUENCES, *Ecological Applications*, 7(3), 737–750, doi:[10.1890/1051-0761\(1997\)007\[0737:HAOTGN\]2.0.CO;2](https://doi.org/10.1890/1051-0761(1997)007[0737:HAOTGN]2.0.CO;2), 1997.
- Wang, S., Hong, Y., Wu, J., Xu, X.-R., Bin, L., Pan, Y., Guan, F. and Wen, J.: Comparative analysis of two 16S rRNA gene-based PCR primer sets provides insight into the diversity distribution patterns of anammox bacteria in different
670 environments, *Applied Microbiology and Biotechnology*, 99(19), 8163–8176, doi:[10.1007/s00253-015-6814-8](https://doi.org/10.1007/s00253-015-6814-8), 2015.
- Weiss, R. F.: The solubility of nitrogen, oxygen and argon in water and seawater, *Deep Sea Research and Oceanographic Abstracts*, 17(4), 721–735, doi:[10.1016/0011-7471\(70\)90037-9](https://doi.org/10.1016/0011-7471(70)90037-9), 1970.
- Weiss, R. F. and Craig, H.: Precise shipboard determination of dissolved nitrogen, oxygen, argon, and total inorganic carbon by gas chromatography, *Deep Sea Research and Oceanographic Abstracts*, 20(4), 291–303, doi:[10.1016/0011-7471\(73\)90054-5](https://doi.org/10.1016/0011-7471(73)90054-5),
675 1973.
- Weiss, R. F. and Price, B. A.: Nitrous oxide solubility in water and seawater, *Marine Chemistry*, 8(4), 347–359, doi:[10.1016/0304-4203\(80\)90024-9](https://doi.org/10.1016/0304-4203(80)90024-9), 1980.
- Welti, N., Bondar-Kunze, E., Mair, M., Bonin, P., Wanek, W., Pinay, G. and Hein, T.: Mimicking floodplain reconnection and disconnection using ¹⁵N mesocosm incubations, *Biogeosciences*, 9(11), 4263–4278, doi:[10.5194/bg-9-4263-2012](https://doi.org/10.5194/bg-9-4263-2012), 2012.
- 680 Wenk, C. B., Bles, J., Zopfi, J., Veronesi, M., Bourbonnais, A., Schubert, C. J., Niemann, H. and Lehmann, M. F.: Anaerobic ammonium oxidation (anammox) bacteria and sulfide-dependent denitrifiers coexist in the water column of a meromictic south-alpine lake, *Limnology and Oceanography*, 58(1), 1–12, doi:[10.4319/lo.2013.58.1.0001](https://doi.org/10.4319/lo.2013.58.1.0001), 2013.
- Wenk, C. B., Zopfi, J., Gardner, W. S., McCarthy, M. J., Niemann, H., Veronesi, M. and Lehmann, M. F.: Partitioning between benthic and pelagic nitrate reduction in the Lake Lugano south basin, *Limnology and Oceanography*, 59(4), 1421–
685 1433, doi:[10.4319/lo.2014.59.4.1421](https://doi.org/10.4319/lo.2014.59.4.1421), 2014.



- Williams, W. D.: Environmental threats to salt lakes and the likely status of inland saline ecosystems in 2025, *Environmental Conservation*, 29(2), 154–167, doi:[10.1017/S0376892902000103](https://doi.org/10.1017/S0376892902000103), 2002.
- Xue, Y., Yu, Z., Chen, H., Yang, J. R., Liu, M., Liu, L., Huang, B. and Yang, J.: Cyanobacterial bloom significantly boosts hypolimnetic anammox bacterial abundance in a subtropical stratified reservoir, *FEMS Microbiology Ecology*, 93(fix118),
690 doi:[10.1093/femsec/fix118](https://doi.org/10.1093/femsec/fix118), 2017.
- Yang, J., Jiang, H., Wu, G., Hou, W., Sun, Y., Lai, Z. and Dong, H.: Co-occurrence of nitrite-dependent anaerobic methane oxidizing and anaerobic ammonia oxidizing bacteria in two Qinghai-Tibetan saline lakes, *Frontiers of Earth Science*, 6(4), 383–391, doi:[10.1007/s11707-012-0336-9](https://doi.org/10.1007/s11707-012-0336-9), 2012.
- Yoon, S., Nissen, S., Park, D., Sanford, R. A. and Löffler, F. E.: Nitrous Oxide Reduction Kinetics Distinguish Bacteria
695 Harboring Clade I NosZ from Those Harboring Clade II NosZ, edited by J. E. Kostka, *Appl. Environ. Microbiol.*, 82(13), 3793, doi:[10.1128/AEM.00409-16](https://doi.org/10.1128/AEM.00409-16), 2016.
- Zilius, M., Vybernaite-Lubiene, I., Vaiciute, D., Petkuvienė, J., Zemlys, P., Liskow, I., Voss, M., Bartoli, M. and Bukaveckas, P. A.: The influence of cyanobacteria blooms on the attenuation of nitrogen throughputs in a Baltic coastal lagoon, *Biogeochemistry*, 141(2), 143–165, doi:[10.1007/s10533-018-0508-0](https://doi.org/10.1007/s10533-018-0508-0), 2018.

700

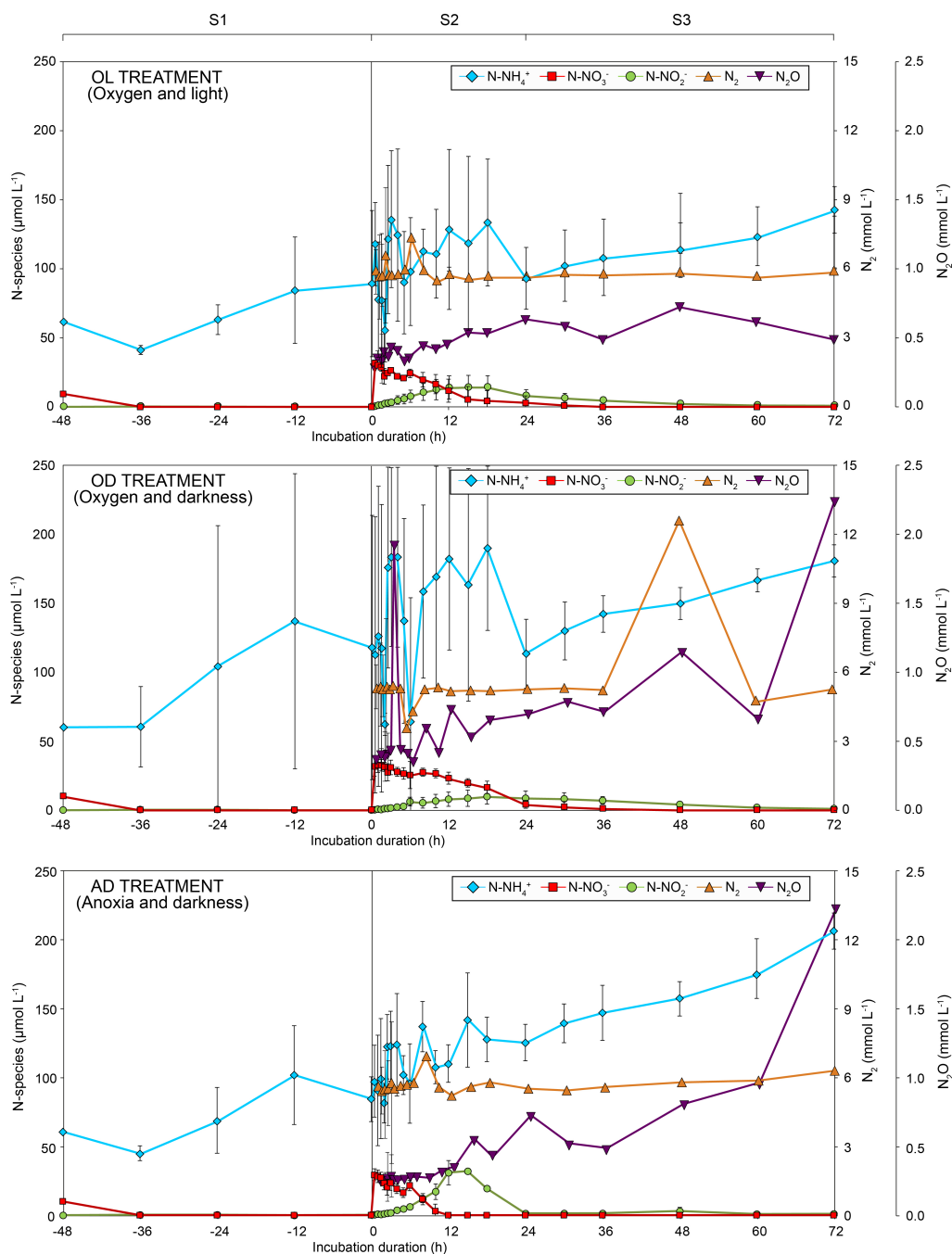


Figure 1: Inorganic N species evolution over time in the three studied treatments. Nitrate (NO₃⁻), nitrite (NO₂⁻), ammonium (NH₄⁺), dinitrogen gas (N₂) and nitrous oxide (N₂O) evolution over time. Three different stages could be distinguished during incubations: a first stage (S1) extended from sampling (NC₋₄₈) to ¹⁵N-NO₃⁻ addition (time 0 h), the second stage (S2) covered the time between 0 and 24 h, and the third stage (S3) from time 24 h to the end of incubation (time 72 h). The negative times indicate the stabilization period. ¹⁵N-NO₃⁻ was added at 0 h. S1, S2, and S3 refer to the three stages distinguished during incubations. Error bars represent ± 1 standard deviation.

705

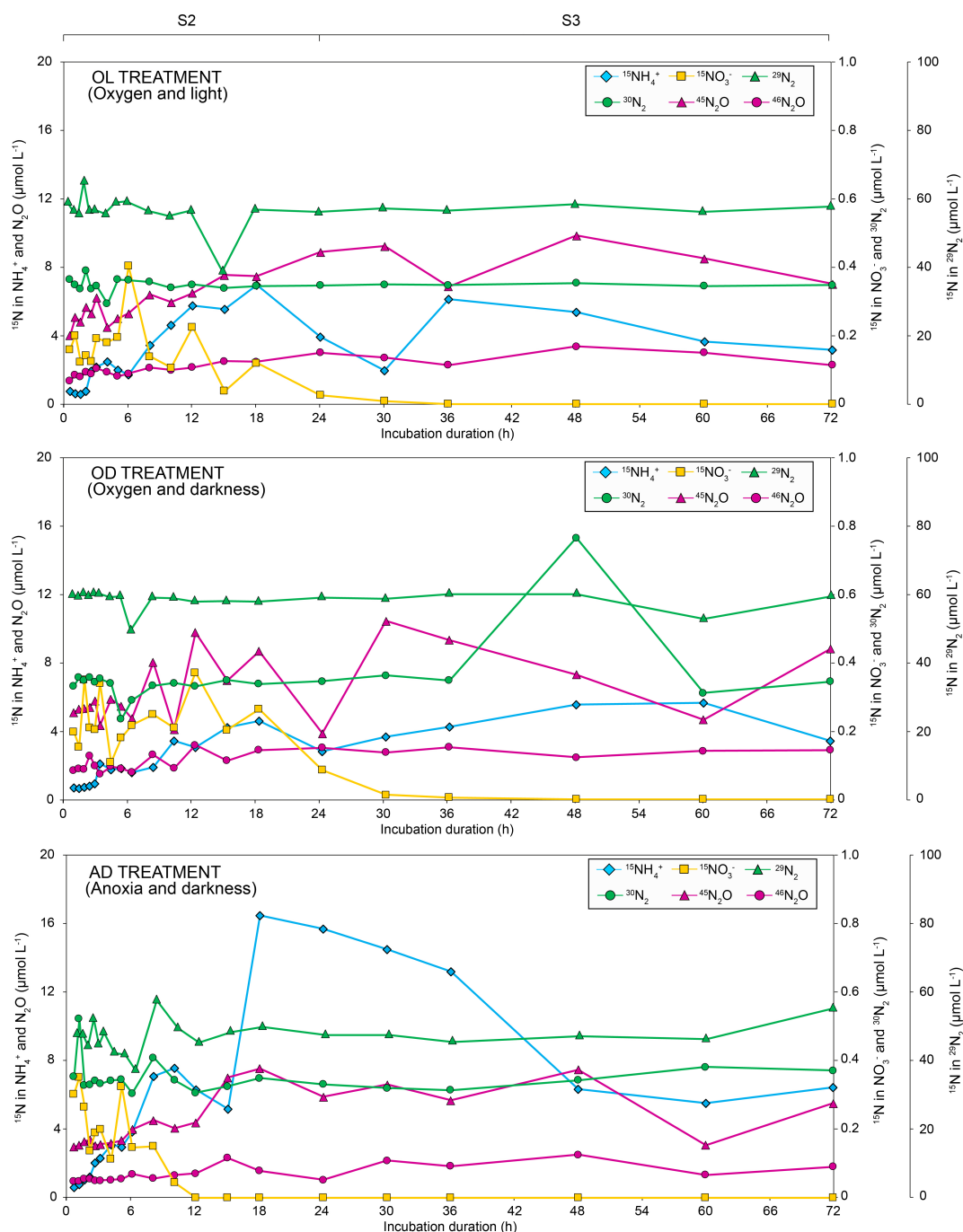
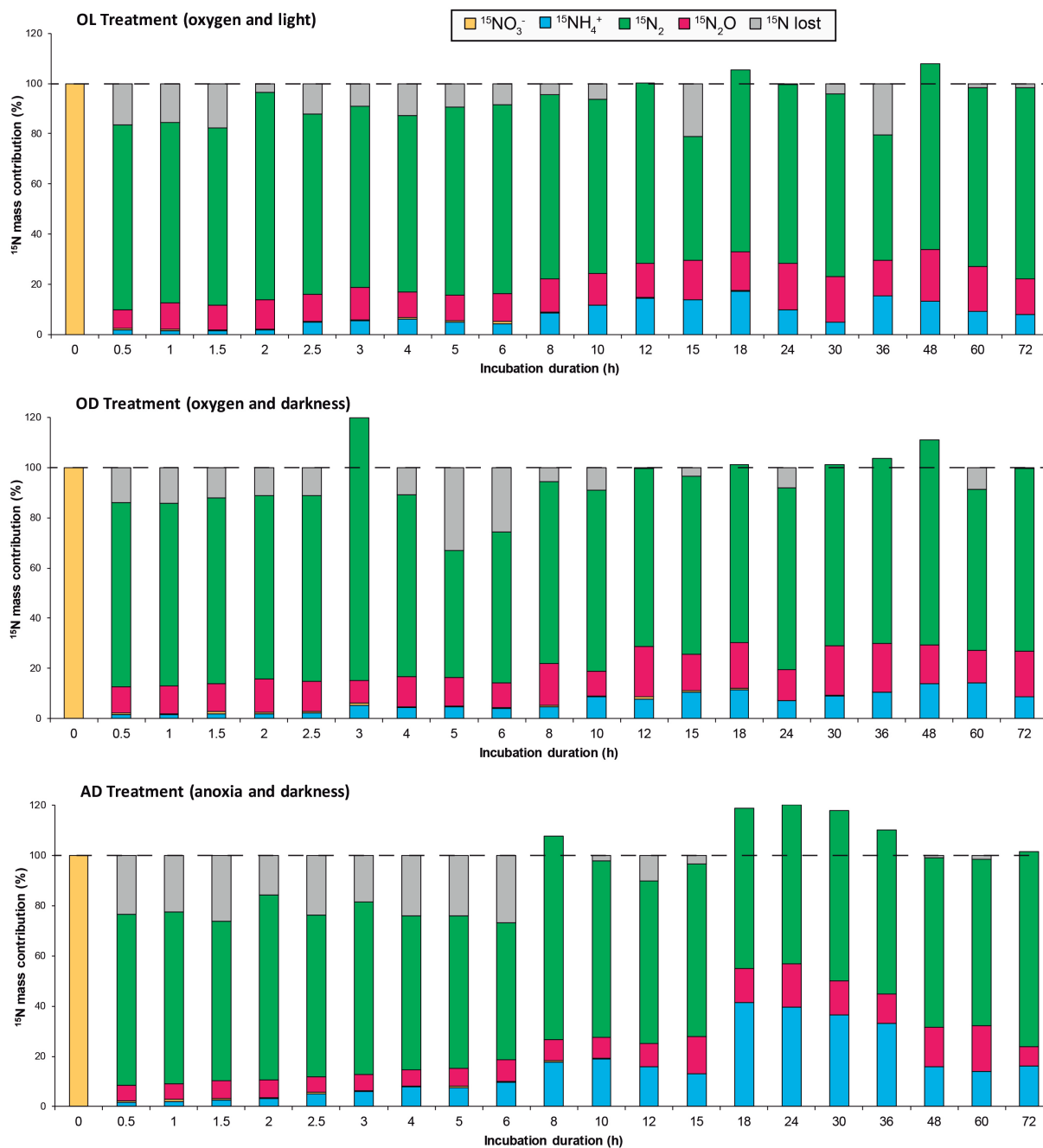


Figure 2: ^{15}N evolution over time. Evolution of $^{15}\text{NH}_4^+$, $^{15}\text{NO}_3^-$, $^{29}\text{N}_2$, $^{30}\text{N}_2$, $^{45}\text{N}_2\text{O}$ and $^{46}\text{N}_2\text{O}$ concentration from the $^{15}\text{N}\text{-NO}_3^-$ addition. It includes second stage (S2; 0 - 24 h) and third stage data (S3; 24 - 72 h).



710 **Figure 3: Mass balance of ^{15}N during incubation time in the three treatments. Percentage of ^{15}N recovery in $^{15}\text{NH}_4^+$, $^{15}\text{NO}_3^-$, $^{15}\text{N}_2$ (including $^{29}\text{N}_2$ and $^{30}\text{N}_2$), and $^{15}\text{N}_2\text{O}$ (including $^{45}\text{N}_2\text{O}$ and $^{46}\text{N}_2\text{O}$) at each time point for the three treatments of the study.**

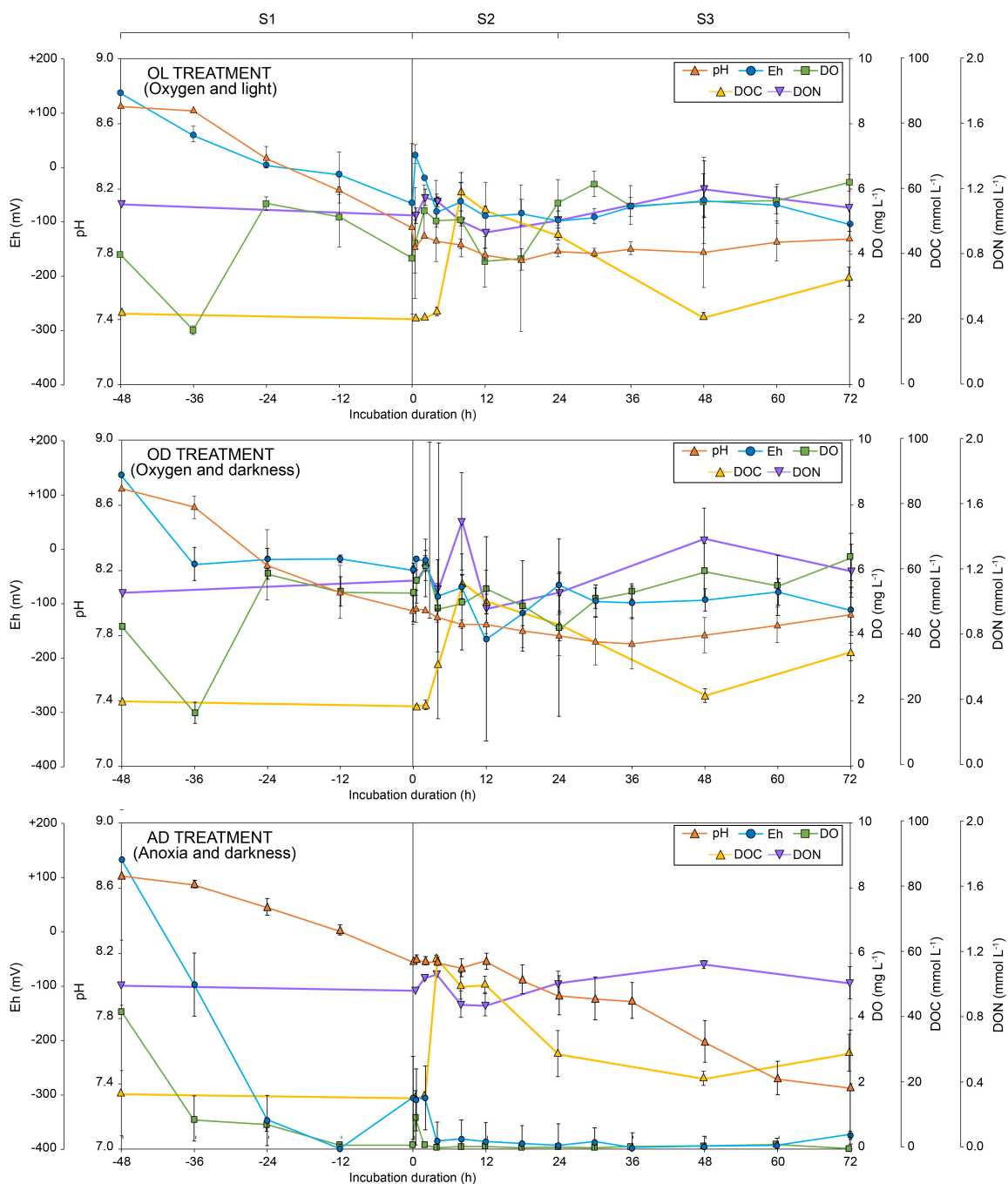


Figure 4: Physical-chemical, DOC, and DON evolution over time. pH, redox potential (Eh), dissolved oxygen (DO), dissolved organic carbon (DOC), and dissolved organic nitrogen (DON) evolution over time in the three studied treatments (OL, OD, and AD). The negative times indicate the stabilization period. Error bars represent ± 1 standard deviation.

715

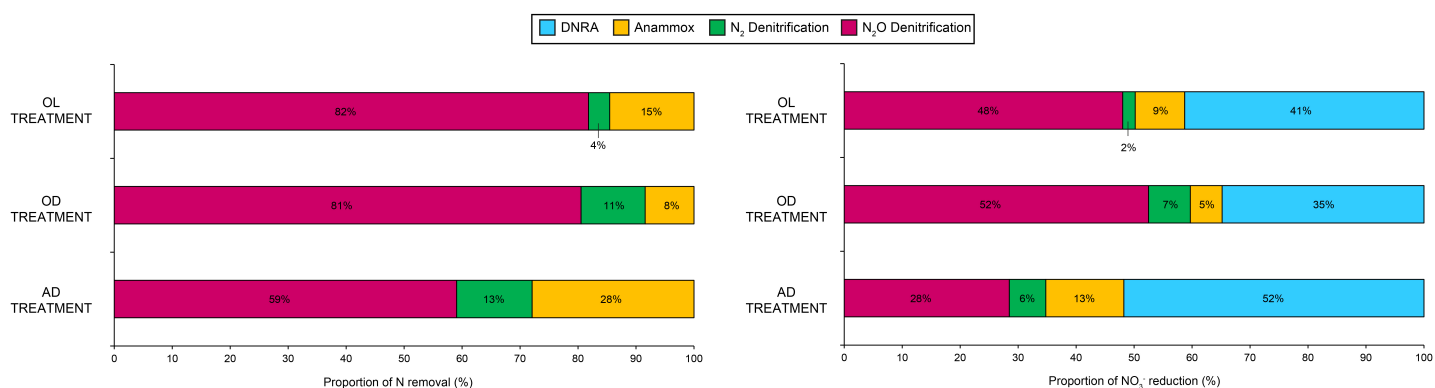


Figure 5: Contribution of each pathway to total nitrogen removal and nitrate reduction. Proportion of N₂-denitrification, N₂O-denitrification, and anammox to total N removal (left). Contribution of DNRA, N₂-denitrification, N₂O-denitrification, and anammox to nitrate reduction (right). Rates were measured at three different incubation conditions (treatments OL, OD, and AD).

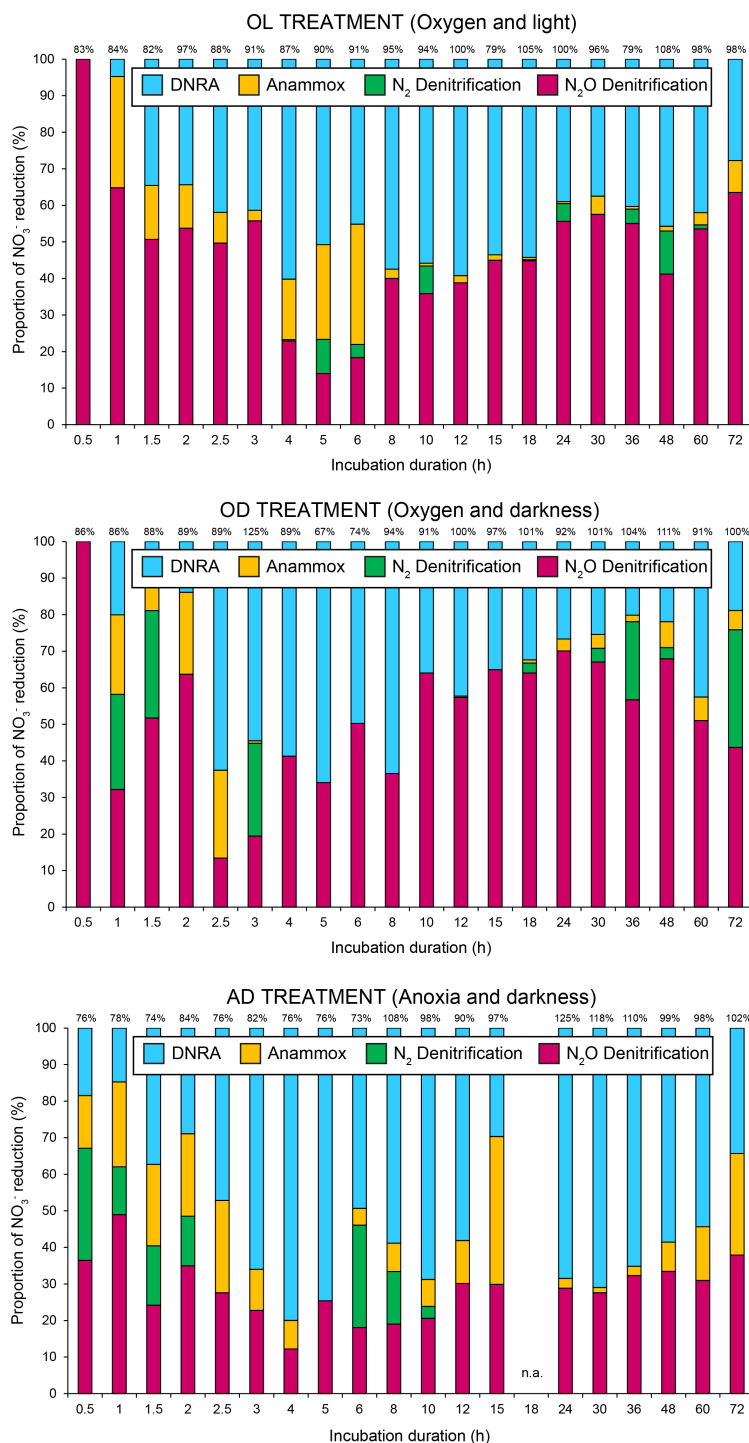


Figure 6: Evolution of the contribution to nitrate reduction processes over time. Proportion of N₂-denitrification, N₂O-denitrification, DNRA, and anammox over time under three incubation conditions (treatments OL, OD, and AD). Proportions of each process were measured at twenty different incubation times, by triplicate per treatment. Recovery percent of the initial ¹⁵N at each time is shown above the bars. Detailed mass balance is included in Figure S2. n.a.: not available.



Table 1. Parameters and equations used in the ¹⁵N-IPT modeling based on Salk et al. (2017).

Parameter	Description	Equation
P_{29}	²⁹ N ₂ production (measured directly)	
P_{30}	³⁰ N ₂ production (measured directly)	
P_{45}	⁴⁵ N ₂ O production (measured directly)	
P_{46}	⁴⁶ N ₂ O production (measured directly)	
r_{14}	¹⁴ N/ ¹⁵ N ratio in NO ₃ ⁻ (measured directly)	
r_{14a}	¹⁴ N/ ¹⁵ N ratio in NH ₄ ⁺ (measured directly)	
P_{15-NH4}	¹⁵ NH ₄ ⁺ production (measured directly)	
D_{28}	²⁸ N ₂ production via denitrification	$r_{14}^2 \cdot (P_{30} - A_{30})$
D_{29}	²⁹ N ₂ production via denitrification	$2r_{14} \cdot (P_{30} - A_{30})$
D_{30}	³⁰ N ₂ production via denitrification	$P_{30} - A_{30}$
A_{28}	²⁸ N ₂ production via anammox	$(r_{14} \cdot A_{29}) / [(r_{14}/r_{14a}) + 1]$
A_{29}	²⁹ N ₂ production via anammox	$P_{29} - D_{29}$
$A_{29-DNRA}$	²⁹ N ₂ production via coupled DNRA-anammox	$A_{29} / [1 + (r_{14}/r_{14a})]$
$A_{29-Anammox}$	²⁹ N ₂ production via canonical anammox	$A_{29} - A_{29-DNRA}$
A_{30}	³⁰ N ₂ production via anammox	$(P_{29} - 2P_{30} \cdot r_{14}) / (r_{14a} - r_{14})$
D_{14}	N ₂ genuine production via denitrification	$2D_{28} + D_{29}$
D_{14-N2O}	N ₂ O genuine production via denitrification	$r_{14} \cdot (2P_{46} + P_{45})$
A_{14}	N ₂ genuine production via anammox	$2A_{28} + A_{29-DNRA}$
$A_{14-DNRA}$	N ₂ genuine production via coupled DNRA-anammox	$A_{29-DNRA} + 2A_{28} \cdot (A_{29-DNRA} / A_{29})$
$A_{14-Anammox}$	N ₂ genuine production via canonical anammox	$2A_{28} \cdot (A_{29-Anammox} / A_{29})$
P_{14}	Total N ₂ + N ₂ O genuine production	$D_{14} + A_{14} + D_{14-N2O}$
$DNRA$	NH ₄ ⁺ genuine production via DNRA	$r_{14} \cdot (P_{15-NH4} + A_{30})$



Table 2. Mean values (\pm SD) of physico-chemical parameters in water and sediment for the experiments at the beginning and at the end of incubations.

Treatment	Conditions water column	pH	Eh (mV)	DO (mg/L)	EC (mS/cm)	TDS (g/L)	DOC (mmol L ⁻¹)	DNb (mmol L ⁻¹)	DON (mmol L ⁻¹)
OL ₇₂ (n=3)	Aeration and light	7.89 \pm 0.08	-105.7 \pm 28.1	6.46 \pm 0.26	75.9 \pm 3.90	45.5 \pm 3.30	27.0 \pm 2.9	1.12 \pm 0.17	0.98 \pm 0.16
OD ₇₂ (n=3)	Aeration and darkness	7.93 \pm 0.13	-114.3 \pm 41.0	6.40 \pm 0.73	76.8 \pm 0.86	47.1 \pm 0.56	31.3 \pm 2.6	1.30 \pm 0.15	1.12 \pm 0.15
AD ₇₂ (n=3)	Anoxia and darkness	7.40 \pm 0.35	-370.7 \pm 7.51	0.08 \pm 0.02	80.9 \pm 0.91	50.1 \pm 0.80	28.7 \pm 5.7	1.21 \pm 0.08	1.01 \pm 0.09

Treatment	DON:DNb (%)	N-NO ₃ (μ mol L ⁻¹)	N-NH ₄ (μ mol L ⁻¹)	N-NO ₂ (μ mol L ⁻¹)	N ₂ (mmol L ⁻¹)	N ₂ O (mmol L ⁻¹)	LOI (%)	S-N-NO ₃ (μ mol kg ⁻¹)	S-N-NH ₄ (mmol kg ⁻¹)	S-N-NO ₂ (μ mol kg ⁻¹)
OL ₇₂ (n=3)	87.5 \pm 0.5	BLD	139 \pm 15.7	BLD	6.07 \pm 0.28	0.52 \pm 0.05	8.84 \pm 1.56	68.4 \pm 13.4	0.60 \pm 0.27	BLD
OD ₇₂ (n=3)	86.4 \pm 1.7	BLD	175 \pm 10.9	BLD	5.88 \pm 0.02	2.28 \pm 2.69	8.51 \pm 1.46	64.6 \pm 24.4	1.22 \pm 0.76	BLD
AD ₇₂ (n=3)	83.5 \pm 2.0	BLD	198 \pm 12.2	BLD	6.27 \pm 0.74	2.23 \pm 3.09	9.90 \pm 1.31	73.2 \pm 16.0	1.83 \pm 0.27	BLD

(*) At NC₄₈: n = 1 in water samples for determination of all the chemical parameters; n = 3 in sediment samples (LOI, S-N-NO₃⁻, S-N-NH₄⁺, and S-N-NO₂⁻). Eh: redox potential. DO: dissolved oxygen. EC: electrical conductivity. TDS: total dissolved solids. DOC: dissolved organic carbon. DNb: dissolved bound nitrogen. DON: dissolved organic nitrogen. LOI: loss of ignition. BLD: below limit of detection. n.a.: not available.



Table 3. Mean (\pm SD) and maximum rates of N-loss processes after 72 h of mesocosm incubations.

Mesocosms	N-conversion rates ($\text{mmol N m}^{-2} \text{h}^{-1}$)															
	Total N removal		Total NO_3^- reduction		N_2 -Denitrification		N_2O -Denitrification		DNRA-Anammox		Canonical Anammox		N_2 -Anammox		DNRA	
	mean	max	mean	max	mean	max	mean	max	mean	max	mean	max	mean	max	mean	max
OL-1 (n=20)	2.22 (\pm 2.13)	6.88	3.72 (\pm 3.26)	10.5	0.13 (\pm 0.25)	0.85	1.85 (\pm 1.92)	6.89	0.17 (\pm 0.34)	1.10	0.07 (\pm 0.12)	0.42	0.24 (\pm 0.46)	1.52	1.50 (\pm 1.57)	5.01
OL-2 (n=20)	2.16 (\pm 3.42)	12.3	3.46 (\pm 4.35)	15.9	0.00 (\pm 0.02)	0.07	1.39 (\pm 3.13)	12.3	0.55 (\pm 0.86)	2.49	0.22 (\pm 0.40)	1.26	0.77 (\pm 1.24)	3.38	1.29 (\pm 1.25)	3.65
OL-3 (n=20)	2.29 (\pm 2.62)	9.78	4.09 (\pm 3.92)	15.1	0.03 (\pm 0.11)	0.46	2.03 (\pm 2.69)	9.78	0.15 (\pm 0.45)	1.66	0.09 (\pm 0.25)	0.78	0.24 (\pm 0.70)	2.45	1.80 (\pm 1.76)	5.59
OL (n=60)	2.23 (\pm 2.71)	12.3	3.76 (\pm 3.79)	15.9	0.05 (\pm 0.16)	0.85	1.76 (\pm 2.58)	12.29	0.29 (\pm 0.61)	2.49	0.12 (\pm 0.28)	1.26	0.41 (\pm 0.88)	3.38	1.54 (\pm 1.53)	5.59
OD-1 (n=20)	1.54 (\pm 2.10)	7.65	2.30 (\pm 2.10)	7.65	0.10 (\pm 0.28)	1.00	1.43 (\pm 2.15)	7.65	0.00 (\pm 0.01)	0.05	0.00 (\pm 0.01)	0.04	0.01 (\pm 0.02)	0.09	0.76 (\pm 0.79)	2.01
OD-2 (n=20)	2.54 (\pm 2.56)	11.0	4.33 (\pm 3.36)	15.4	0.08 (\pm 0.17)	0.70	1.70 (\pm 1.55)	5.31	0.41 (\pm 0.88)	3.62	0.36 (\pm 0.87)	3.34	0.77 (\pm 1.72)	6.96	1.79 (\pm 1.36)	4.41
OD-3 (n=20)	4.35 (\pm 4.73)	14.7	5.73 (\pm 4.92)	16.7	1.03 (\pm 2.59)	8.33	3.07 (\pm 2.68)	9.81	0.14 (\pm 0.57)	2.48	0.11 (\pm 0.47)	2.05	0.25 (\pm 1.04)	4.53	1.38 (\pm 1.16)	3.94
OD (n=60)	2.87 (\pm 3.51)	14.7	4.22 (\pm 3.89)	16.7	0.41 (\pm 1.57)	8.33	2.10 (\pm 2.24)	9.81	0.20 (\pm 0.64)	3.62	0.17 (\pm 0.60)	3.34	0.37 (\pm 1.22)	6.96	1.35 (\pm 1.20)	4.41
AD-1 (n=20)	4.52 (\pm 6.00)	21.0	7.41 (\pm 8.12)	25.3	0.00 (\pm 0.00)	0.00	4.40 (\pm 6.00)	21.0	0.08 (\pm 0.30)	1.33	0.04 (\pm 0.15)	0.66	0.12 (\pm 0.45)	1.99	2.89 (\pm 3.12)	13.9
AD-2 (n=20)	3.18 (\pm 5.64)	19.7	6.16 (\pm 6.14)	22.1	1.79 (\pm 3.93)	13.0	0.40 (\pm 1.12)	4.96	0.66 (\pm 1.51)	5.73	0.33 (\pm 0.66)	1.84	0.99 (\pm 2.12)	7.54	2.98 (\pm 2.21)	8.68
AD-3 (n=20)	3.16 (\pm 4.21)	13.5	5.68 (\pm 5.28)	19.7	0.58 (\pm 1.95)	8.17	0.75 (\pm 1.07)	3.97	0.80 (\pm 1.37)	5.36	1.02 (\pm 2.26)	7.26	1.82 (\pm 3.48)	11.0	2.53 (\pm 2.36)	8.64
AD (n=60)	3.63 (\pm 5.30)	21.0	6.43 (\pm 6.56)	25.3	0.80 (\pm 2.61)	13.0	1.87 (\pm 3.99)	21.0	0.51 (\pm 1.21)	5.73	0.46 (\pm 1.38)	7.26	0.96 (\pm 2.40)	11.0	2.80 (\pm 2.56)	13.9



Table 4. Published rates of sedimentary denitrification, DNRA and anammox measured in intact sediment cores ($\text{mmol N m}^{-2} \text{h}^{-1}$). n.a.: not available

Source	DNRA	Anammox	N ₂ -Denitrification	N ₂ O-Denitrification	Reference
Pétrola Lake (Spain)	0 - 2.800	0 - 0.960	0 - 0.800	0 - 2.100	This study
Colne estuary (United Kingdom)	0.005 - 0.400	0.157	n.a.	n.a.	Dong et al. (2009)
Cisadane estuary (Indonesia)	1.140	n.a.	n.a.	n.a.	Dong et al. (2011)
Thau lagoon (France)	6.708	n.a.	n.a.	n.a.	Gilbert et al. (1997)
East China Sea shelf (China)	0.791 - 3.583	n.a.	n.a.	n.a.	Song et al. (2013)
Fringing marsh-aquifer ecotone (USA)	0.875 - 6.125	n.a.	1.800 - 17.60	n.a.	Tobias et al. (2001)
Plum Island Sound estuary (USA)	0.004 - 0.310	n.a.	0 - 0.332	n.a.	Koop-Jakobsen and Giblin (2010)
German Bight (Germany)	0.010	n.a.	0.124	n.a.	Marchant et al. (2016)
Heron Island (Australia)	n.a.	n.a.	0.034 - 0.480	n.a.	Eyre and Ferguson (2008)
Lake Tanganyika (Burundi, DRC, Tanzania, Zambia)	n.a.	0.100	n.a.	n.a.	Schubert et al. (2006)
Randers Fjord (Denmark)	n.a.	0.014 - 0.021	0.219 - 0.335	n.a.	Risgaard-Petersen et al. (2004)
Thames estuary (United Kingdom)	n.a.	0 - 0.010	0.036 - 0.155	n.a.	Trimmer et al. (2003)
Gravesend, Thames estuary (United Kingdom)	n.a.	0.049	0.193	n.a.	Trimmer et al. (2006)
Constructed wetland in New South Wales (Australia)	n.a.	0.066 - 0.199	0.652 - 0.966	n.a.	Erler et al. (2008)
Taihu Lake (China)	n.a.	0.049 - 0.413	0.132 - 0.656	n.a.	Han and Li (2016)
Lake Superior (Canada, USA)	n.a.	0.021 - 0.040	0.019 - 0.128	n.a.	Crowe et al. (2017)
Danshuei estuary (Taiwan)	n.a.	0.013	0.126	0.050	Hsu and Kao (2013)
Pearl River estuary (China)	n.a.	0 - 0.003	0.032 - 0.708	0 - 0.022	Tan et al. (2019)
Lake Bonney (Antarctica)	n.a.	n.a.	n.a.	0.191	Prisu et al. (1996)
Tuven and Divar, Goa (India)	n.a.	n.a.	n.a.	0.140 - 0.670	Fernandes et al. (2010)
Pantanal wetland (Brazil)	n.a.	n.a.	n.a.	0 - 1.560	Lienggaard et al. (2014)
Ashtamudi estuary (India)	n.a.	n.a.	n.a.	0.490 - 4.850	Salahudeen et al. (2018)